

12-2012

Performance Evaluation of Video Streaming in an Infrastructure Mesh Based Vehicle Network

Sajindra Pradhananga
Clemson University, sajindra.sp@gmail.com

Follow this and additional works at: https://tigerprints.clemson.edu/all_theses

 Part of the [Electrical and Computer Engineering Commons](#)

Recommended Citation

Pradhananga, Sajindra, "Performance Evaluation of Video Streaming in an Infrastructure Mesh Based Vehicle Network" (2012). *All Theses*. 1516.

https://tigerprints.clemson.edu/all_theses/1516

This Thesis is brought to you for free and open access by the Theses at TigerPrints. It has been accepted for inclusion in All Theses by an authorized administrator of TigerPrints. For more information, please contact kokeefe@clemson.edu.

PERFORMANCE EVALUATION OF VIDEO STREAMING IN AN INFRASTRUCTURE MESH BASED VEHICLE NETWORK

A Thesis
Presented to
the Graduate School of
Clemson University

In Partial Fulfillment
of the Requirements for the Degree
Master of Science
Electrical Engineering

by
Sajindra B. Pradhananga
December 2012

Accepted by:
Dr. Kuang-Ching Wang, Committee Chair
Dr. Harlan B. Russell
Dr. John Komo

Abstract

Most next-generation wireless networks are expected to support video streaming which constitutes the bulk of traffic on the Internet. This thesis evaluates the performance of video streaming in a vehicle network with an infrastructure wireless mesh network (WMN) backhaul. Several studies have investigated video quality performance primarily in single hop wireless networks and static WMNs. This thesis is based on those studies and conducts the study in relation to a network where the multi-hop features of the mesh network and mobility of the streaming clients may have substantial impact on the perceived video quality in the network.

The study assumes a previously proposed vehicle network architecture consisting of an infrastructure WMN that serves as the mesh backhaul [2, 3]. A number of mesh routers (MRs) form the mesh backhaul using one of their two IEEE 802.11g radios whereas the other radio is used to communicate with the fast moving mesh clients (MCs). Selective MRs called mesh gateways (MGs) are connected to a wired network (e.g., the Internet, hereafter referred to as the core network) via a point-to-point link and provide gateway connectivity to the rest of the network. A server on the core network acts as a video server and streams individual video streams to the fast moving MCs. Upon deployment, network discovery occurs and segregates the network into a number of separate routing zones with each routing zone consisting of a single MG and all the MRs that use the MG as their gateway. A minimum-hop

based routing protocol is used to enable seamless handover of MCs from one MR to another within a single zone.

Simulation studies in this thesis inspects the network and video streaming performance within a single routing zone, assuming the handoff and inter-zone routing being taken care of by the routing protocol and only focus on the intra-zone packet forwarding and scheduling impacts. Hence, this study does not address cases where MCs move from one routing zone to another routing zone in the mobile network. In the first part of the study, we evaluate the performance of video streaming in the described network by studying performance metrics across different layers of the protocol stack. The number of video flows that can be supported by the network is experimentally determined for each scenario. In the second part, the thesis studies controllable network and protocol parameters' ability to improve the network and video quality performance. Simulations are run in an integrated framework that includes network-simulator ns-2, NS-MIRACLE, and Evalvid.

Dedication

I would like to dedicate this thesis to my loving wife, family and friends whose support have guided me in every phase of my life.

Acknowledgments

First and foremost, I would like to thank my advisor, Dr. Kuang-Ching Wang for all the guidance and support he provided throughout my graduate study at Clemson. The discussions I've had with him have always provided me with insight and guided me in the right direction in my research. I would also like to take this opportunity to thank Dr. Harlan B. Russell and Dr. John Komo for their guidance and serving on my thesis committee.

I would also like to especially thank Dr. Daniel Noneaker for his support along with the ECE faculty and my fellow ECE graduate students.

Table of Contents

Title Page	i
Abstract	ii
Dedication	iv
Acknowledgments	v
List of Tables	viii
List of Figures	ix
1 Introduction	1
2 Related Work and Background	6
2.1 Related Work	6
2.2 Background	8
3 Network Model	16
3.1 Initial Discovery	17
3.2 Routing	19
4 Simulation Framework	23
4.1 Network Simulation	23
4.2 Video Evaluation Framework	24
4.3 Simulation Parameters	26
5 Results	33
5.1 Performance Evaluation	34
5.2 Change in Contention Window	41
5.3 Video Packet MTU Variation	47
6 Conclusions and Future Work	51
Appendices	53

A	Simulation Framework Setup	54
	Bibliography	56

List of Tables

2.1	MOS rating	12
2.2	PSNR to MOS conversion	15
4.1	Simulation parameters	28
4.2	Encoded video parameters	30

List of Figures

2.1	GOP structure	10
3.1	Network topology	17
3.2	Routing zones	19
4.1	Evalvid framework	24
4.2	Chain network topology	27
4.3	Protocol architecture for different node types	29
4.4	Sample frame from mother daughter clip used for simulation	30
4.5	Bit-rate profile of mother daughter clip	31
4.6	PSNR profile of mother daughter clip	31
5.1	Throughput vs. number of video flows	35
5.2	MAC layer packet loss vs. number of video flows	35
5.3	CDF of end-to-end frame delay	37
5.4	End-to-end frame loss vs. number of video flows	38
5.5	Average PSNR vs. number of video flows	39
5.6	Average MOS vs. number of video flows	39
5.7	Distribution of frames with different MOS vs. number of video flows	40
5.8	Proportion of frames with different MOS values	41
5.9	Throughput for CW change scenario	42
5.10	MAC layer packet loss for CW change scenario	43
5.11	Frame loss for CW change scenario	44
5.12	CDF for end-to-end frame delay CW change scenario	45
5.13	PSNR for CW change scenario	45
5.14	MOS for CW change scenario	46
5.15	Distribution of frames with different MOS for CW change scenario	46
5.16	Comparison between original and CW change scenario	47
5.17	Throughput vs. number of video flows (2048 bytes MTU)	48
5.18	Throughput vs. number of video flows (512 bytes MTU)	48
5.19	Average MAC layer packet loss (2048 bytes MTU)	48
5.20	Average MAC layer packet loss (512 bytes MTU)	48
5.21	CDF for end-to-end frame loss (2048 bytes MTU)	49
5.22	CDF for end-to-end frame loss (512 bytes MTU)	49
5.23	End-to-end frame loss (2048 bytes MTU)	50

5.24	End-to-end frame loss (512 bytes MTU)	50
5.25	PSNR vs. number of flows (2048 bytes MTU)	50
5.26	PSNR vs. number of flows (512 bytes MTU)	50
5.27	MOS vs. number of flows (2048 bytes MTU)	50
5.28	MOS vs. number of flows (512 bytes MTU)	50

Chapter 1

Introduction

The rapid proliferation of wireless networks has enabled end users to have access to Internet at places such as airports, coffee shops or parks away from the comfort of home or offices; however, users now expect ubiquitous broadband access especially when mobile. Mobile broadband access, especially from vehicles, increases the comfort and productivity of passengers and there is a market for infotainment applications such as television, gaming, multimedia streaming etc. in vehicles [35].

Currently, cellular networks are the primary means of broadband access when mobile; however they require relatively expensive and data-capped contract based subscriptions for end users. Especially, with consumption of multimedia content in the form of audio and video streaming becoming one of the most important applications on the Internet, data-capped cellular contracts are not really ideal for media consumption for the end user.

As an alternative, generic IEEE 802.11 based wireless local area networks (LANs) can be deployed quickly and efficiently, are cost effective to establish and maintain but have small coverage areas. For example, [30] introduced the idea of Drive-thru Internet where IEEE 802.11b based wireless LAN (WLAN) was leveraged

to provide network access for mobile users particularly on highway scenarios. Many studies have been carried out in recent years to extend such wireless LANs to cover larger area by means of various technologies. Wireless mesh networks (WMNs), one of the key technologies for next-generation wireless networking [1], have been identified as cost-effective and easily deployable solutions for providing coverage in a wide area [6, 34]. Self-configuration, low upfront deployment costs and self healing capabilities [36] have made WMNs as more attractive and robust propositions to other alternative types of wide area network (WAN) wireless technologies and has led to growing adoption in the wireless networking community.

The deployment of any such next-generation wireless network is heavily dependent on the network's ability to support an array of emerging and demanding end user applications such as multimedia streaming, online gaming, real-time video communications. The consumption of media content, especially video streaming, is growing at a very fast pace and is predicted to constitute almost 90% of the total global consumer Internet traffic by 2015 [14]. Hence, WMNs also must be able to support such services to be commercially feasible as well.

Supporting video streaming in wireless networks represents a very challenging task as compared to wired networks. In wired networks, the high Quality of Service (QoS) requirements of video traffic such as high bandwidth, stringent delay and jitter can be readily satisfied by using high bandwidth-capable, low-delay and reliable media and by over-provisioning. On the other hand, the wireless medium is inherently less reliable and has less capacity than its wired counterpart. Moreover, the wireless channel is highly dynamic and more prone to interference which may fail with strict QoS requirements of video traffic.

The study of video streaming over wireless networks has received much attention from the research community over the past few years [7, 8, 9, 10, 11, 38, 23, 24,

32, 33, 40]. Performance improvement and evaluation studies are the two main topics of research in this area. Initial studies on video streaming in wireless networks were carried out in relation to single hop IEEE 802.11b/g WLANs. In [11], the authors studied the performance of unicast video streaming over a single WLAN with respect to the background traffic. In [32], the performance of video and voice traffic was studied in multi-hop wireless networks but the mesh network was set up in ad-hoc mode instead of infrastructure mode which is more suited to any practical or commercial deployment. More importantly, the evaluation was done in terms of network layer metrics only.

Performance evaluation studies of video streaming in mobile infrastructure WMN based networks has hardly been reported. Performance analysis of video streaming in mesh networks is essential for a clear understanding of application and network characteristics in such complex networks and to facilitate robust protocol design in the future. Factors such as multi-hop transmissions further complicate the issues in wireless networks by elevating chances of cross-interference and reduced system capacity and thus, providing video streaming services over WMNs is a very challenging issue. A better understanding of the relationships that exist between video quality and network/link layer metrics will help in robust protocol design and any form of network capacity planning for practical deployments.

In this thesis, the performance evaluation of video streaming in a WMN based vehicle network resembling a highway based vehicle network deployment has been carried out. The study considers a previously proposed network architecture consisting of an IEEE 802.11g based infrastructure WMN deployed along a highway serving video streams to a number of mobile clients (MCs) in the architecture [2, 3]. A number of mesh routers (MRs) are deployed along potential paths that the mobile clients are most likely to travel. A few MRs, known as Mesh Gateways (MGs), are connected

to a wired network (e.g., the Internet, hereafter referred to as the core network) via backhaul links and provide gateway connectivity. Any MC that enters the network initiates network connections and association with the network and as it moves along maintains persistent connection with the network. The implemented routing mechanism along with MobileIP ensures that an MC can perform seamless handover as it moves through the network.

The main objective of this thesis is to experimentally evaluate the video quality and network metrics with respect to the number of video flows in the described network. It begins with the implementation of a simulation framework that enables us to capture the characteristics of video streaming in mobile environments. The study conducted all simulations within one single routing zone in the described architecture, omitting the handoff and inter-zone routing issues while focusing on the packet forwarding and scheduling performance within one single zone. For the studied network architecture, the congestion at the gateway was found to be a major deterrent to support a larger number of flows in the network. Although, video quality in general is dependent upon the delay, jitter and packet loss, the study observed that the packet loss in the system has more influence on the perceived video quality in this network than the end-to-end delay. At the same time, the throughput and frame loss rate are also analyzed to investigate the relationship with the video quality metric. The impact of varying network and protocol parameters such as the contention window and packet size on the network performance has also been investigated.

The rest of the thesis is organized as follows. Chapter 2 discusses related work and provides a brief background on video encoding and video quality metrics. The simulation framework and the video evaluation framework have also been discussed in Chapter 2. Chapter 3 discusses the network architecture and the intra-zone routing mechanism used to facilitate seamless handover within a single zone. Chapter 4 dis-

cusses the simulation framework. Results have been discussed in Chapter 5. Chapter 6 concludes the study and identifies areas for possible future study.

Chapter 2

Related Work and Background

2.1 Related Work

Most of the existing literature on video streaming in wireless networks can be broadly classified into two types of studies viz. a) performance improvement studies and b) performance evaluation studies. In performance improvement studies, mechanisms varying from application layer approaches such as streaming rate adaptation to link and physical layer approaches such as link rate and channel resource allocation have been used to optimize video streaming [9, 16, 17, 23, 32]. In [39], optimization of video streaming was studied using source rate adaptation, packetization and error control. In [25] and [41], retransmission, channel resource allocation and forward error control mechanisms were used to deal with high packet loss and delay variation in wireless networks. Cross-layer optimization schemes is also a prevalent theme in many optimization studies [4, 5, 15, 16, 20, 22, 26, 27]. In [19] and [31], application level information is used to optimize the network and MAC layer parameters such as transmission link rates, retransmission policy, packet scheduling policy as well as setting up IEEE 802.11e priorities.

On the performance evaluation side as well, there has been a number of experimental studies of video streaming in different types of networks [23, 38, 32, 11, 24, 10, 8, 40, 7, 9, 33]. In [11], the performance of unicast video streaming with respect to the background traffic was studied. It was seen that an increase in packet rates and decrease in packet size of the background traffic resulted in greater degradation in the quality of the video being streamed. However, in this study, only a single hop scenario using IEEE 802.11b was addressed and the evaluation of video quality was done in terms of a network layer metric only. In [24], weather forecasts based on WLAN characteristics such as RSSI, and link capacity were used to predict streaming video quality. In both these cases, the study has been carried out in single-hop WLANs only. In [32], an experimental testbed based study is conducted for a multi-hop mesh network where the impact of different traffic and network characteristics such as RTS/CTS, MAC layer retransmission counts etc. are studied on video performance. However, the study was done for a mesh network in an ad-hoc mode and focused only on network layer metrics. Ad-hoc mode WMNs are less suited to practical and commercial deployments than infrastructure-based WMNs.

More significantly, in [11, 32], it was seen that the studies did not evaluate the video quality using an application layer metric but instead considered metrics such as packet latency, packet loss and packet jitter enough to characterize the quality of video transmission. However, it is a well-acknowledged fact that such network layer metrics do not have a unique and universal relationship with the perceived video quality.

Study of video streaming in mesh networks were carried out in [9, 32]. In [9], the authors experimented on real networks and used peak signal-to-noise ratio (PSNR) as the application evaluation metric. It was seen that the PSNR depended on the number of streams and lower number of hops resulted in higher average PSNR

values. However, the study was carried out in a WMN with all nodes being static. Video streaming in mobile scenarios have been studied in [7, 40]. In [7], network congestion is shown to greatly impact the quality of video streaming in vehicular networks and a solution that utilizes frame skipping and transcoding along with frame rate reduction techniques over IEEE 802.11 networks is shown. However, the networks used in this study are ad-hoc networks and do not utilize the benefit of infrastructure WMNs. Also in [40], inter-vehicular video streaming is studied using the dedicated short-range communications (DSRC) protocol instead of IEEE 802.11b/g.

Multi-hop and mobile architecture presented in our study varies significantly in terms of network characteristics as compared to single hop networks or even static multi-hop networks. Hence, it is important from a research and commercial point of view that such network architecture be studied to realize issues that are not seen in general studies. Also, most of these studies focus on new protocols or enhancements and do not provide a clear reference as to how existing technology behaves in such networks. Our objective is to develop an environment to study existing technologies such as IEEE 802.11b/g in such networks and see how far we are from using the base IEEE MAC protocol in such networks.

2.2 Background

This section presents a brief overview of MPEG-4 encoding, video quality evaluation metrics and the framework used for this evaluation.

2.2.1 MPEG-4 Basics

The video format used for our study is MPEG4, the video codec standard defined by the Motion Picture Experts Group. MPEG-4 is one of the most widely used

video encoding/decoding standards developed by Motion Picture Experts Group in collaboration with the International Telecommunication Union as the successor to the MPEG-1 and MPEG-2 standards. The MPEG-4 specification also defines standards for multimedia content storage and delivery in addition to the encoding/decoding standards. Like all other video codecs, the MPEG-4 specification does not specify any design of the encoder but rather specifies just the syntax for encoding. The following section briefly gives an overview of the MPEG-4 standard and basics of video encoding.

2.2.2 MPEG-4 Encoding

Raw uncompressed video generally requires very high transmission bandwidth and hence is highly unsuitable for transmission without any form of compression. The MPEG-4 standard like other encoding/decoding standards intends to efficiently compress and decompress the video in order to lower the transmission bandwidth requirement for videos. Also, MPEG-4 is a lossy codec meaning that the video resulting from encoding and subsequent decoding doesn't match the quality of the original video completely. The higher the compression rate, the higher is the deviation or loss from the original video quality.

All modern video encoding/decoding methods take advantage of spatial and temporal redundancy to compress data in source videos. Any video can be considered as a series of consecutive images called frames. Each frame can be thought of consisting of a number of equally sized blocks called macro-blocks usually 8x8 pixels or 16x16 pixels in size. All encoding schemes are generally applied to these macro-blocks instead of the entire frame and the sizes of macro-blocks may also vary from one compression scheme to the other. Spatial redundancy exists due to high correla-

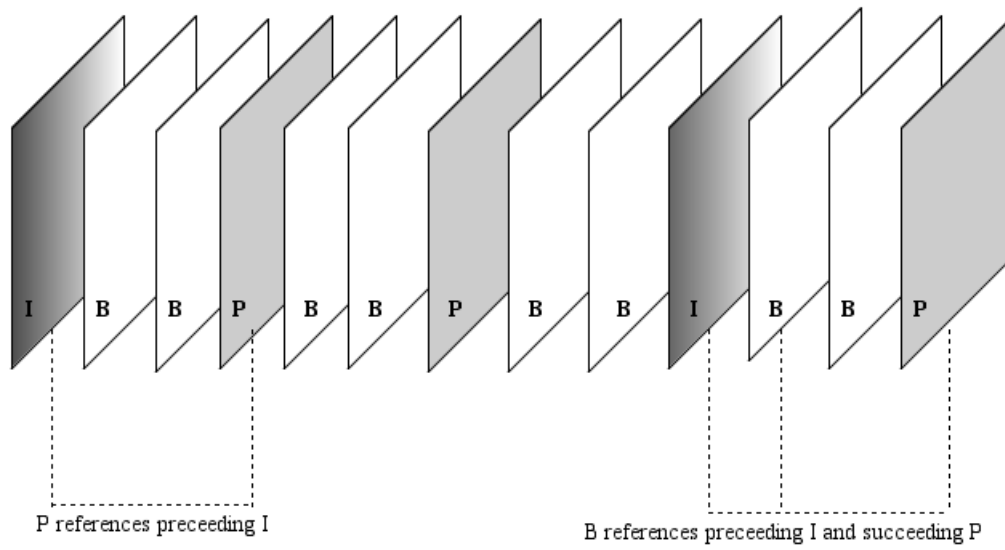


Figure 2.1: GOP structure

tion between adjacent data points in a single frame whereas temporal redundancy is due to the high correlation between consecutive frames in a video. In almost all the videos, even in videos with motion, two consecutive frames are very similar allowing compression methods to store the redundant data just once and then only storing differential data for successive frames. Modern image compression algorithms and file formats such as the JPEG format make use of spatial redundancy reduction methods. On the other hand, temporal redundancy is generally reduced by storing only differential data for two consecutive frames and is known as inter-frame coding or inter-coding. Motion estimation, motion compensated prediction are different types of widely used inter-frame coding methods. Compression achieved using inter-frame coding in general is much higher than using intra-frame coding.

The MPEG-4 standard also makes use of intra-frame and inter-frame coding mechanisms and defines three types of frames in the encoded video viz. I, P and B frames. An I-frame also known as a key frame is the result of intra-coding performed

within a single frame without any other frame as a reference. P-frames are predicted frames that exploit both spatial and temporal redundancy and contain intra-coded parts along with motion vectors determined using the process of motion estimation. These motion vectors use previous I-frames or P-frames as reference. B-frames (bidirectionally predicted frames) exploit only temporal redundancy and use both previous and later frames (I or P) for reference. Hence, an I frame can be decoded at the receiving end independently and P frames can only be decoded completely if the previous I or P frame is available. Successfully decoding a B frame requires the availability of both the previous and successive I or P frame. I-frames and P-frames are the only frames that can be used as reference frames for encoding other types of frames and B-frames are never used for that purpose. Fig. 2.2.2 shows the basic structure of an MPEG-4 encoded video.

All the frames in MPEG-4 encoded video are arranged in a structure called a Group of Pictures (GOP). A GOP can be considered as the most basic unit of an encoded video with the video stream consisting of a series of GOPs. The basic structure of a GOP has been illustrated in Figure 2.2.2. Each GOP consists of exactly one I-frame at the start of the GOP followed by P frames which have been predicted on the basis of the I-frame in the GOP. B-frames are optional and may or may not be present in the GOP structure. Once set, the length of the GOP and the structure of a GOP in an encoded video stream is usually fixed. In any GOP, the I frame is the largest in size because they carry the most information. Hence, any loss of an I-frame means maximum loss of information in a GOP. Moreover, as all the remaining P-frames have been coded with the I-frame as a reference, I-frame's loss also affects the succeeding P-frames i.e. if an I frame is lost, the impact propagates over to the rest of the frames in the same GOP. The loss of a P frame only affects the related B-frames whereas a B-frame's loss doesn't affect any other frame as such.

MOS	Quality	Impairment
5	Excellent	Imperceptible
4	Good	Perceptible but not annoying
3	Fair	Slightly annoying
2	Poor	Annoying
1	Bad	Very Annoying

Table 2.1: MOS rating

2.2.3 Video Evaluation Metrics

Video content transmission is one of the most challenging content distribution frameworks. In addition to already discussed stringent QoS requirements on the network, it is also challenging to reliably and quickly obtain a metric that correlates well to the end user’s perception of a video’s quality. In a video distribution framework, the end users’ perspective of a video is deemed as the most reliable form of assessing video quality. This method of evaluating a video’s quality by a survey of end users is generally termed as subjective evaluation. The mean opinion score (MOS) is such a subjective quality metric that is determined by surveying a number of end users about the quality of the video and has been regarded as the most reliable video quality metric. The MOS is generally represented by a score from 1 to 5 with 1 representing the worst perceived video quality and 5 the best perceived video quality. An ITU-R developed quality scale with respect to MOS scores that is deemed to correlate well with video quality as perceived by the human eye is presented in Table 2.1.

Despite their high correlation with the video quality as perceived by the Human Visual System (HVS), subjective video quality metrics are impractical, expensive and most importantly time consuming to be used for any sort of video quality evaluation. Hence, objective video quality metrics have been developed over the years to determine the video quality quickly and to be used in real world evaluations where

they can be generated automatically. These objective video quality metrics take into account any sort of disparity between the original video and the possibly distorted received video. For each pixel, the absolute difference between the reference video and the degraded video is calculated and then translated into a score, that represents the video quality, using various statistical methods. Various popular metrics such as Mean Square Error (MSE), Signal to Noise Ratio (SNR), Peak Signal to Noise Ratio (PSNR) etc. are based upon such statistical analysis of absolute pixel differences. Of these, PSNR stands out as one of the most widely used video quality metrics and is known to correlate better than SNR to video quality as perceived by the human eye.

Peak-Signal-to Noise Ratio is the most widely used objective video quality metric. It is a differential metric derived from SNR and compares the maximum possible energy to the noise energy in a single image. It is defined by the eq.

$$PSNR = 10 * \log_{10} * \frac{10(2^M - 1)^2}{MSE} \quad (2.1)$$

where MSE refers to the Mean Squared Error and is defined by

$$MSE = \frac{1}{m * n} \sum_{i=0}^{m-1} \sum_{j=0}^{n-1} [I(i, j) - K(i, j)]^2 \quad (2.2)$$

where I and K refer to two monochrome images sized $m*n$.

Objective metrics like PSNR have the obvious advantages of being relatively simple, easier and faster to calculate; however, one of the key drawbacks with these types of metrics is that they may not correlate well with subjective quality (as perceived by the human eye) under certain conditions. For example, PSNR being a differential metric, it makes PSNR values of a received video only valid if the original transmitted video had a high subjective metric based score in the first place. It may always not be the case hence this condition must be satisfied while using PSNR as a

quality metric. In general, it has been seen that under the condition a high quality video is used as a reference in PSNR measurement, a PSNR value above 40dB indicates that the test video is also of high quality. Values below 30dB indicate videos of lower quality. Also, PSNR is not a reliable measure of quality across different video contents, but it has been shown that PSNR is reliable within the content itself. It is meaningless to ascertain the quality of a received video using PSNR values by comparing it with the original which itself was "poor" in terms of video quality.

Hence, the change in PSNR values is a dependable indicator of the variation in quality of a video provided the following conditions are met:

- The content is fixed
- The codec is fixed
- The original/reference video itself is of high subjective quality

For the purpose of our study, we use PSNR metric as an intermediate step in our evaluation process with MOS as the main performance metric. The main reasons behind our adoption of PSNR for our study lies in:

- relatively quick and simple calculation of PSNR and it's continued prevalent use,
- conformation to condition that the original video must have high MOS keeps PSNR metric still valid , and
- most importantly, the presence of a widely accepted heuristic mapping of PSNR to MOS. In [18], a widely accepted and used heuristic mapping of PSNR to MOS values which correlates well with human eye perception of videos with relatively

PSNR [dB]	MOS
>37	5 (Excellent)
31-37	4 (Good)
25-31	3 (Fair)
20-25	2 (Poor)
<20	1 (Bad)

Table 2.2: PSNR to MOS conversion

low motion has been proposed. The mapping table has been presented in Table 2.2.

Chapter 3

Network Model

The network model considered in this study was previously proposed in [2, 3] as illustrated in Fig 3.1. It models an IP based infrastructure WMN composed of a number of mesh routers (MRs) that behave as access points and provide network access to a number of mobile mesh clients (MCs). A few selected MRs are also connected to the core network by means of backhaul links and provide gateway services to the network in addition to acting as access points. These MRs are specifically called mesh gateways (MGs). Any reference to MRs hereafter also includes the MGs. Each MR is equipped with two IEEE 802.11b/g radios operating in orthogonal channels. One of the radios is used for communicating with other MRs whereas the other radio is used for communicating with the MCs. Orthogonality of the two channels is implemented to ensure minimal cross-channel interference. All the MCs move along the roadside and keep on communicating persistently with the mesh network. Each MC streams a video from a video server present in the core network.

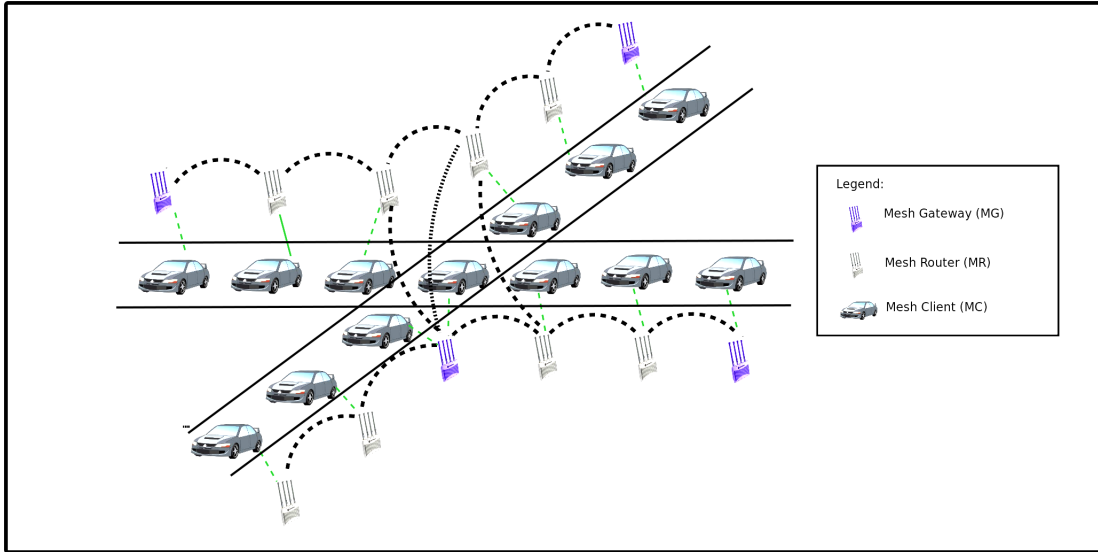


Figure 3.1: Network topology

3.1 Initial Discovery

Upon initial deployment, each MR engages in the process of mesh formation via network discovery. We refer to the process of establishing a multi-hop routing path from every MR in the system to its nearest MG as Network Discovery. The following sequence of events ensure that the backbone network eventually converges and each MR has a route to the nearest MG in the network.

Each MR including MG advertises itself on the network by flooding the network with a broadcast message. The broadcast advertisement has three key fields:

- SourceID (SRC-ID)
- NextHopID (NH)
- Hopcount (HC)

The SourceID is the address of the node that initially sent the advertisement. The NextHopID is the address of the node that forwarded the advertisement. The

NextHopID is initially set to the same as SourceID. The HopCount indicates the number of hops the recipient node is away from the SourceID. It is set to 1 in the original advertisement from each MR.

Any node that receives an advertisement checks to see if it has a route to the address specified in SRC-ID. Three possible cases exist

- If the node doesn't have any such route, it adds a route to SRC-ID with NH as the next-hop towards the node and HC as the hopcount. The recipient node then forwards the advertisement again after setting itself as NH and incrementing HC by 1.
- If the node already has a route, it uses lowest HC as the metric to determine the best route. If the newer route is better than the existing route, the routing table is updated and the MR forwards the advertisement in a manner similar to the first case.
- If the existing route is better than the newer route, the advertisement is dropped.

As a consequence of the above procedure, any node that receives an advertisement directly from another node will add a route and always forward the advertisement. If any node receives multiple copies of the broadcast message from different neighboring senders, it uses the hop count to determine the best route. Flooding is controlled by setting the maximum hop-count limit, which guarantees a packet will not be transmitted more than the maximum number of hops. The advertisement sent from an MG has one additional field set GW in the advertisement. This allows other MRs in the network to identify an advertisement from MGs present in the network. Each MR chooses the closest MG as it's gateway towards the core network.

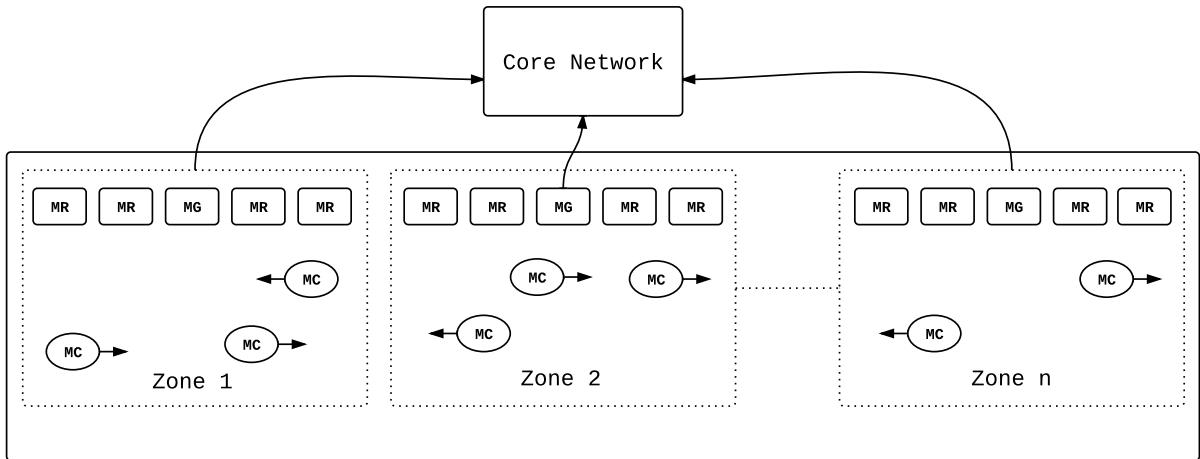


Figure 3.2: Routing zones

3.2 Routing

The initial discovery enables each MR to discover other MRs and MGs in the vicinity most likely through multiple hops. Also, more importantly, each MR also discovers its best route to reach the core network by means of one of the MGs. The entire mesh network then becomes distinctly split into several routing zones as seen in Fig. 3.2, with each zone consisting of a single MG and all the MRs whose best route to reach the core network is via that MG.

Hence, initial network discovery results in the following entries in the routing table for each MR

- Routes to all the MRs in the same zone.
- Route to the gateway (MG) for the zone.

The MCs are mobile nodes which move randomly across the network. As MCs traverse through the network, each MC communicates persistently with the network

by handing over from one MR to another. There are two routing issues in the studied network architecture that need to be addressed to achieve this purpose:

- Routing within a single zone (Intra-zone routing)
- Routing across multiple zones (Inter-zone routing)

When a MC moves within a zone only, the routing mechanism that handles seamless handover from one MR to another inside the zone is termed as intra-zone routing. For handling routing across multiple zones or inter-zone routing, MobileIP is chosen. The two routing mechanisms are described in detail in the following sections.

3.2.1 Intra-Zone Routing

The main objective of intra-zone routing is to enable seamless handover for all MCs from one MR to another inside a zone. The movement of a MC into the coverage area of a new MR requires changes in the routing in the backbone as the MC's position must be known to correctly deliver messages.

This is achieved by the routing protocol by maintaining the following key entries in the routing tables in each MR:

- Routes to all the MRs in the same zone.
- Route to the gateway (MG) for the zone.
- Routes to any MCs associated with the MR
- Routes to other MCs associated with other MRs in the same zone

The first two entries are populated by the initial flooding based network discovery mechanism described earlier in the chapter. The latter two entries are populated as follows:

- Each MC upon entry to the network scans the network and associates to the best MR at the MAC level. Each MC upon entry to the network sends out a DHCP request in order to obtain a home address. All APs behave as DHCP relays and the request is ultimately relayed to the DHCP server on the core network via the MG. The DHCP server thereby assigns a home address to the MC.
- The association at layer 2 triggers a cross-layer message to the routing agent on the MC. The routing agent sends a routing message advertising itself to the associated MR. The routing agent on the MR then advertises the route to the MC on the mesh channel via itself. This route advertisement is then used by each MR to learn the route towards the MC. Each MR that updates its table based on the route advertisement also forwards it on the mesh channel.
- As each MC moves in the network, it periodically keeps track of beacons from neighboring MRs with a view to perform handover. Association with a new MR takes place if the average signal-to-interference noise ratio (SINR) observed over a certain pre-defined duration is better than the average SINR observed for the currently associated MR. The routing agent then triggers a routing message in a manner similar to the previous step to the new MR. Another routing message is sent to the previously associated MR to allow the old MR to remove the direct route to the MC. The routing tables are properly updated at both the new MR and the old MR. The new MR broadcasts a routing update message on the mesh channel to inform other MRs in the zone about the update.

3.2.2 Inter-Zone Routing

MobileIP is used to facilitate seamless IP mobility for MCs moving from one zone to another. MobileIP support is enabled with each MG running both home agent and foreign agent services for its intra-MG zone. For clarity in the following discussion, the initial routing zone in which a MC enters is referred to as the "home zone" whereas the zone the MC is transiting to is referred to as the "foreign zone".

Each MC, upon entry to its home zone, is assigned a home address by the home agent running on the corresponding MG to obtain a better route to the core network. The MC is assigned a care-of address (CoA) by the foreign agent which also advertises the CoA to the initial home agent of the MC. Once notified, the home agent redirects buffered and new incoming packets to the MC via the foreign agent through an IP tunnel via the core network. The MC keeps on using the home address with the foreign agent serving as the default gateway for any outgoing packets from the MC.

Chapter 4

Simulation Framework

The framework used for this simulation based study consists of two major components. The first component is the wireless network simulation framework composed of the Network Simulator, ns-2 [28], the multi-rate library [12] and NS-MIRACLE [29]. The second component is a video evaluation framework called Evalvid [37].

4.1 Network Simulation

NS-2 is a discrete event network simulator widely used in networking research. NS-2, in combination with NS-MIRACLE, provides a suitable platform for wireless network simulation. NS-MIRACLE is basically a set of dynamic libraries that can be integrated into ns-2 and provides features such as cross-layer messaging, multiple modules within a single layer of the protocol stack which were utilized in the study. Addition of such features facilitates implementation of multiple interfaces, multiple channels, cross-layer adaptation mechanisms. In addition to NS-MIRACLE, an enhanced 802.11 implementation for ns-2 was used in the form of dei80211mr dynamic libraries. The dei80211mr library adds features namely different transmission rates,

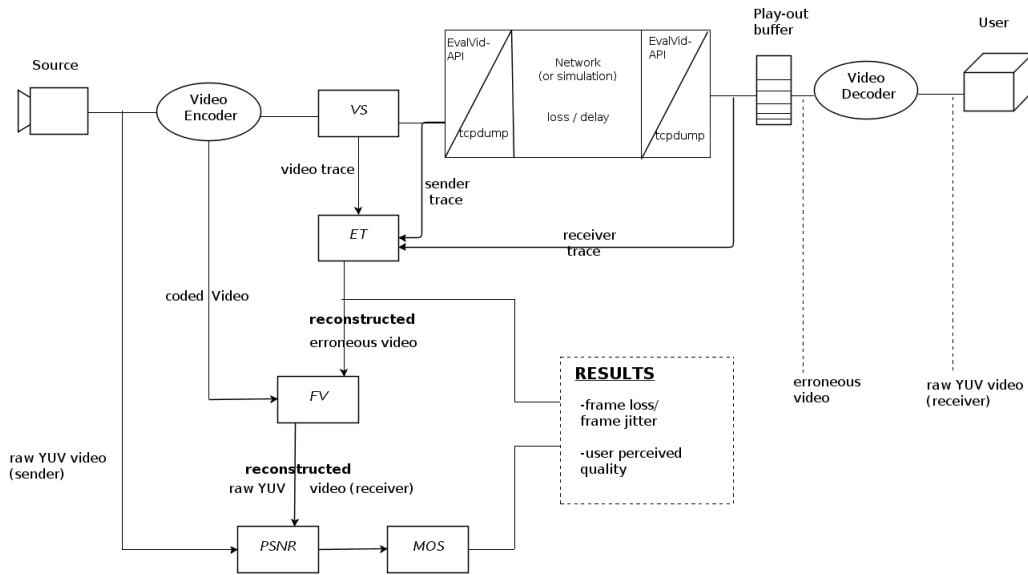


Figure 4.1: Evalvid framework

modulation and coding schemes defined in the IEEE 802.11b/g standard, SINR based packet level error model, link rate adaptation algorithms which assist in realistic simulation of mobile wireless networks. A brief introduction of the libraries and their features have been explained in Appendix A. For detailed understanding of these libraries, readers can refer to [12, 28, 29].

4.2 Video Evaluation Framework

Evalvid is one of the most widely used video evaluation framework that allows us to evaluate the quality of video transmitted over a real or a simulated network with the help of video traces. The metric used for this evaluation is PSNR and Mean Opinion Score (as described in the Chapter 2). The basic architecture of the Evalvid framework is as shown in Fig 4.2 and has been explained in detail in [21].

The steps involved in the evaluation of video quality using this framework can

be outlined as follows:

- Raw video generally in YUV format is first encoded into a compressed stream such as MPEG-4. The other popular encoding formats supported by Evalvid include H.263 and H.264 among other formats. For our study, we've chosen the MPEG-4 simple profile format and ffmpeg [13] was used as the encoding tool.
- The MPEG-4 encoded video stream is then parsed into a traffic trace using the mp4trace tool from the tool-set. A traffic trace is essentially a file containing information about the video bitstream such as frame sizes, frame types, packet segmentation etc. The tool also generates a sender dump file that contains information such as packet ids, timestamps for sent times and packet sizes.
- The sender dump file is used for simulation purposes acting as a video source and after simulation, a corresponding receiver dump for each video stream is generated. The information contained in the receiver dump include the ids, timestamps, order and sizes of packets received.
- Using the sender-receiver pair dump files and the video trace along with the MPEG-4 encoded stream, the etmp4 tool reconstructs the received MPEG-4 bitstream as seen by the receiver.
- The ffmpeg encoder is then used to create reference YUV files for the sent MPEG-4 stream and received MPEG-4 stream. They are termed as "reference YUV" and "received YUV" respectively for clarity in following discussion. The PSNR of reference YUV with respect to the raw video represents the impact of encoding on the quality of the video whereas the PSNR of the received YUV represents the impact of encoding plus network on the quality of the video.

Hence, PSNR of "received YUV" with respect to "reference YUV" is calculated to reflect only the impact of the network on the quality of video.

- The psnr tool from the toolset is then used to calculate the PSNR of the received video with respect to the sent video. The tool also calculates the end-to-end delay, jitter, packet and frame loss percentages.
- The mos tool from the toolset is then used to calculate the average MOS of every received video from the PSNR values obtained in the previous step.

4.3 Simulation Parameters

4.3.1 Topology

As with any network deployment, the actual network topology would be dictated by the deployment location. Chain topologies are ideally suited for networks deployed along interstate highways whereas grid topologies will suit urban deployments better. In either case, the proposed network architecture will be logically divided into a number of disparate routing zones defined in Chapter 3 independent of the topology. All performance analysis is performed in terms of such routing zone.

In this study, we limit ourselves to the study of chain topology for each such routing domain as shown in Fig 4.3.1. The topology consists of M number of fixed MRs at a distance of 200m from each other. In our study, M is set to 5. N number of mobile clients (MCs) move laterally in either directions. Each MC starts off randomly at one of the two ends (randomly chosen) and moves towards the other at a random speed uniformly distributed between 20m/s and 35m/s which represents the typical speed range of vehicles in a highway scenario. Each MC traverses the length of the chain before reversing the direction. The movement of each MC is limited such that

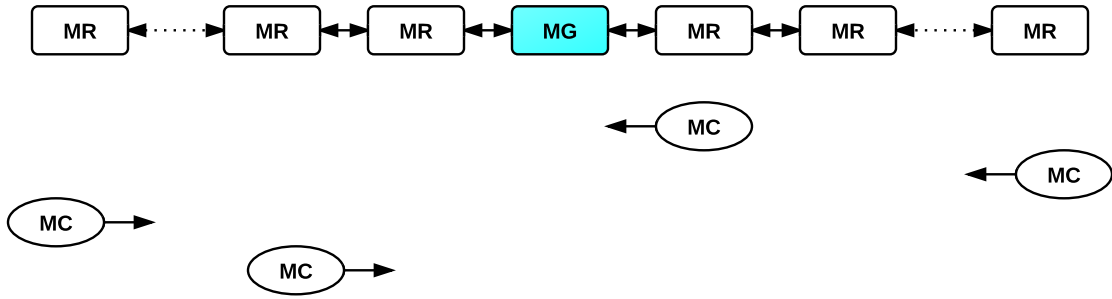


Figure 4.2: Chain network topology

it doesn't go beyond 100m from each end of the topology so that it doesn't move out of the coverage area. Video transmission to each MC starts randomly after it's movement. The MRs form the backbone structure and a number of mobile MCs stream videos downstream from a streaming server connected to the core network.

4.3.2 Link Layer

The 802.11 b/g MAC and PHY layer models introduced by the dei80211mr library were used. Built on top of the standard NS-2 MAC and PHY models, the dei80211mr library introduces several features that were used during the study (Refer to Appendix A). Instead of the traditional NS-2 model where successful packet reception is based on RX Threshold variable, a Signal to Interference Noise Ratio (SINR) based Packet level Error Model has been used. In this model, the Packet Error Rate (PER) is used to determine random packet losses.

The dei80211mr library also supports different link rates and for this study, the link rate for the mesh link was set to 54 Mbps. For the mesh to MC link, the link rate was set to vary according to SNR based link rate adaptation model. The physical layer and noise interference levels were adjusted such that the transmission

<i>Parameter</i>	<i>Value</i>
Slot time	20us
SIFS	20us
DIFS	50us
CWmin	31
CWmax	1023
Retransmission limit	7
Propagation model	TwoRayGround
Carrier Sensing Range	500m
Distance between MRs	200m
DropTail Queue Size	100
Mesh Channel Link Rate	54Mbps
Transmission power	100mw

Table 4.1: Simulation parameters

range is effectively limited to 250 metres. RTS/CTS was not used for the purpose of the study. Other parameters relevant to the simulation have been listed in Table 4.1.

4.3.3 Network Layer

In a mobile scenario, it is essential to detect and react to frequent topology changes. The overall protocol architecture for the MG, MR and MC are as shown in Fig 4.3.3. The routing protocol used within a zone as explained in Chapter 3 has been used.

4.3.4 Application Layer

In many video streaming studies, the application layer is generally complicated with features such as application layer optimization and adaptation schemes. Usually, a video decoder implementation may have a deadline associated with the decoding process, however, in our simulation purposes, no such implementation has been carried out unless mentioned. However, since our focus is mainly on the network and link

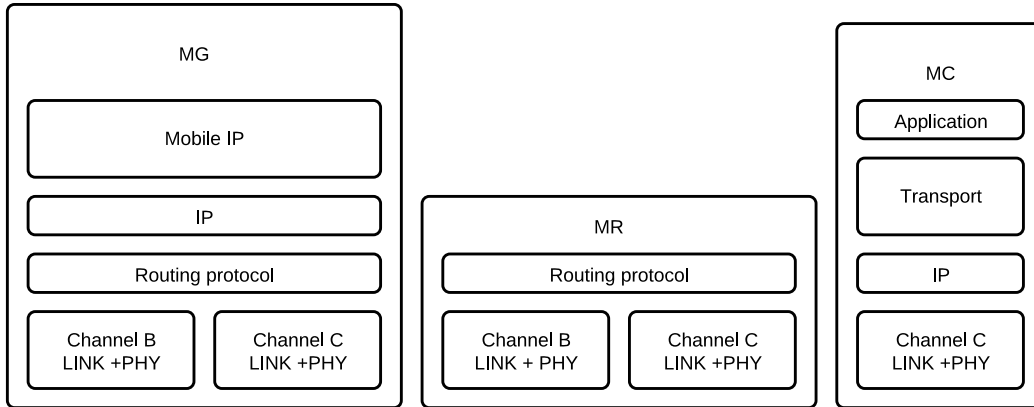


Figure 4.3: Protocol architecture for different node types

layer interactions, the video streaming model considered in our study is a fairly simple one with no specific constraints regarding end-to-end delay and no application layer adaptation or optimization mechanisms at the application level.

In Evalvid, the video files at the receiver are reconstructed using the original video files and the information about lost/late packets/frames. In our study, any frame that has at least one IP packet missing is counted as a lost frame and the lost frame is removed from the video file. The other constraint used in our study is that any packet with a sequence number that is lower than the expected SN is discarded. If any packet arrives with a SN much higher than the expected SN, the packets in between are assumed to have been lost.

4.3.5 Video Parameters

A standard video clip viz. "mother daughter" which has been used by a number of video evaluation studies, were also used for our study. The "mother daughter" clip is a standard low motion video sequence 900 frames long. Table 4.2 lists the relevant video and encoding parameters for the clip.

<i>Parameter</i>	<i>Mother Daughter Clip</i>
Resolution	CIFS (352x288)
No. of frames	900
Frame Rate	30 frames/sec
GOP interval	15
Encoding	MPEG-4
Packet sizes	1024
Average PSNR of encoded video	39.41
Bit-rate	512kbps
No. of packets	2509
MPEG-4 profile	Simple Profile

Table 4.2: Encoded video parameters



Figure 4.4: Sample frame from mother daughter clip used for simulation

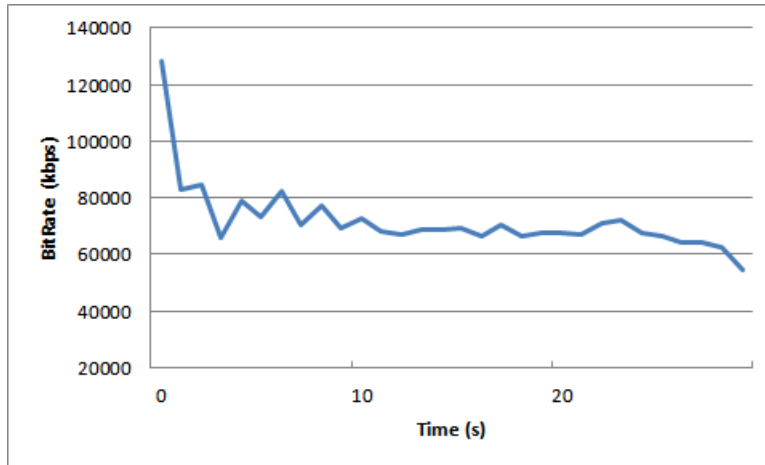


Figure 4.5: Bit-rate profile of mother daughter clip

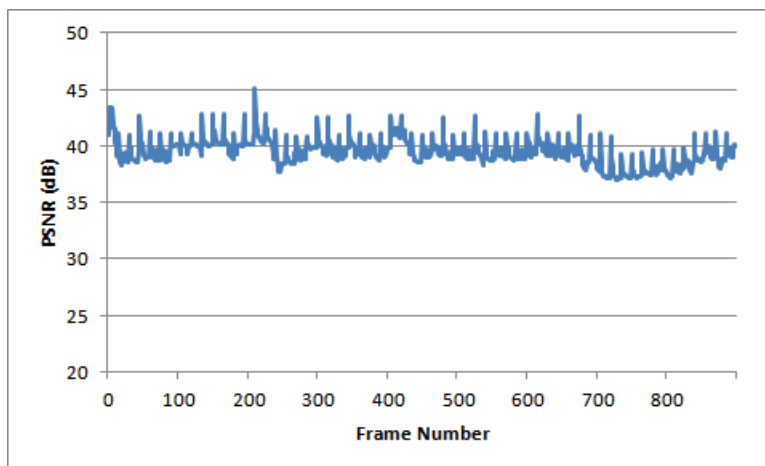


Figure 4.6: PSNR profile of mother daughter clip

Each video was encoded to MPEG-4 format using ffmpeg with a target bitrate of 512kbps with a framerate of 30 frames per second. The GOP interval was set to a length of 30 frames. The snapshot of the video used is as shown in Fig. 4.4. The bitrate profile and the PSNR profile for the clip used are shown in Fig. 4.5 and Fig 4.6 respectively.

Chapter 5

Results

The simulation results presented in this chapter consists of two portions. First, we evaluate the performance of video streaming in the described network architecture with respect to the number of video flows. The maximum number of video flows supported by the network is referred to as the video capacity. In addition to video quality metrics, we also analyze network and link layer metrics such as throughput, end-to-end frame loss and end-to-end frame delay. In the second portion, we evaluate and explain the impact of variation of contention window and application packet size on the perceived video quality and video capacity in the network.

In order to identify the maximum number of video flows supported by the network, we establish a few basic constraints. The PSNR of the transmitted video is 39.41 dB and is equivalent to excellent video quality according to its MOS mapping. So in our study, only scenarios where all received videos with an average MOS in the "good" or "excellent" category (according to Table 2.2) have been accounted towards the supported number of flows in the network. Also, the number of video flows supported by the network in any presented scenario depends on the set of encoded videos, encoding parameters and forwarding mechanisms etc. being used. Even a

slight change in the parameters such as the encoding rate of the video or simply using another video with the same bit-rate would influence the capacity for the presented scenario.

5.1 Performance Evaluation

In the initial scenario, the MCs are randomly placed at one of the two ends of the zone and start moving towards the other end. In our study, each zone consists of a MG with 2 MRs each placed symmetrically on either sides of the MG resulting in 4 mesh links. Each MC streams a video from a video server and streaming to each MC starts within 3-4 seconds of movement. The same video clip was served to each MC in the network. The number of MCs (N) was gradually increased from 4 with each setting repeated 30 times to give meaningful results. Since each MC has only one flow associated with it, N can be used interchangeably with the number of video flows in our study.

Figure 5.1 presents the average throughput measurements for the network with respect to the number of video flows in the network. We define the average traffic rate entering each zone at the MG as the video sending rate. The average combined throughput observed on the mesh-to-mesh links is referred to as the mesh throughput. Similarly, the mesh-to-client throughput refers to the average combined throughput observed on the mesh-to-client links. Fig 5.2 presents the MAC layer packet loss statistics for the two channels.

From Fig 5.1, it can be seen that the average mesh channel and mesh-to-client channel throughput increase as N increases. The network is able to satisfy the average load as the mesh-to-client throughput closely matches the average sending rate for up to $N=16$. At $N=18$, the throughput values start to saturate as the MAC layer

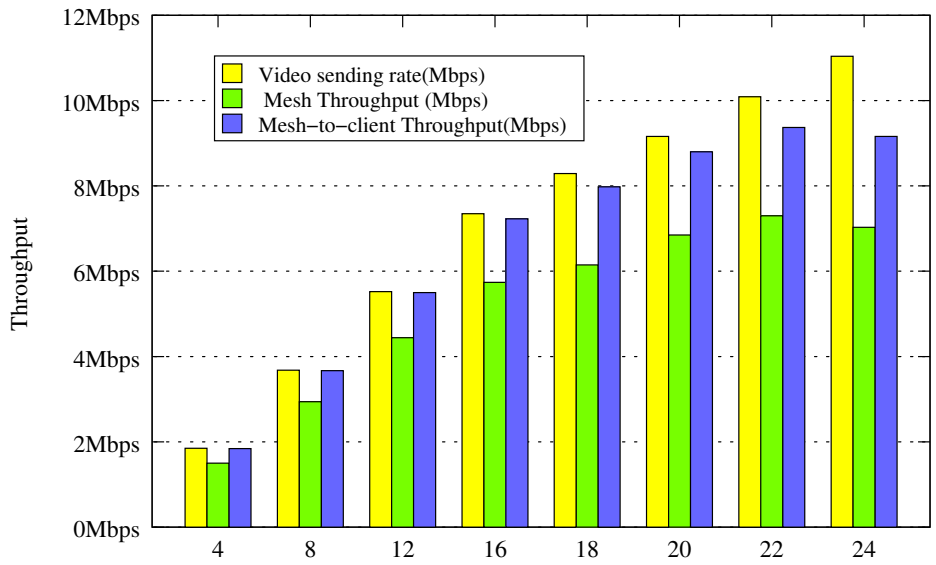


Figure 5.1: Throughput vs. number of video flows

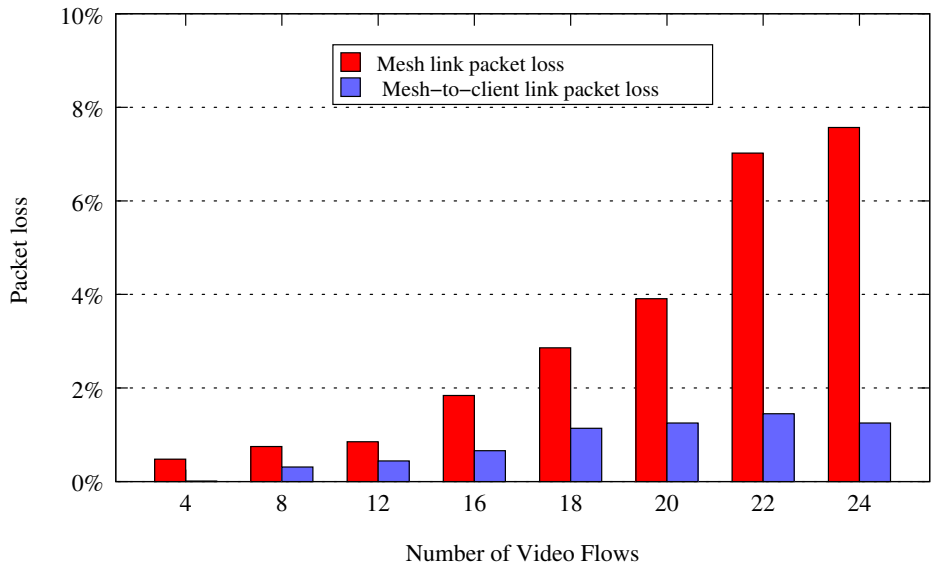


Figure 5.2: MAC layer packet loss vs. number of video flows

packet loss rate increases to 2.86%. More importantly, it was observed that starting at $N=18$ up to $N=22$, more than 90% of the packet drops in the mesh channel was due to queue drops on the MG. When N was increased beyond 22, it was consistently seen that one or more video flows had significant packet losses rendering the decoded video with an unacceptable video quality with MOS below 2. Hence, all calculations from here onwards have been carried out up to $N=22$ only. The figure also indicates that the average mesh throughput lags the average mesh-to-client link throughput. This is because the video traffic for any MC in the coverage region of the MG doesn't need to traverse the mesh network but is directly transmitted from the MG to the corresponding MC.

We also observe that the MAC layer packet loss rate for the mesh channel is consistently higher than that for the mesh-to-client channel. This packet loss graph indicates that the mesh channel saturates well before the client-to-mesh channel and clearly acts as the bottleneck for this network. This arises from the fact that all the traffic aggregates at the MG which increases channel utilization around the MG eventually leading to the MG becoming the bottleneck. This behaviour is generally typical in WMN architectures with prevalent pattern of flows directed either towards or away from the gateway and severely impacts the number of flows that can be supported by the network.

Normally, video quality degradation is mainly caused by two reasons a) packets arriving late and b) packets loss. Most video decoding mechanisms have a deadline within which a packet needs to arrive. Packets arriving after the deadline are simply discarded and hence it is important for packets to arrive in time. Generally, for video streaming the end-to-end frame or packet deadlines are in the order of 1-2 seconds. Fig 5.3 shows the Cumulative Distribution Function (CDF) for end-to-end frame delay. In all observations, the end-to-end frame delay is observed for successfully

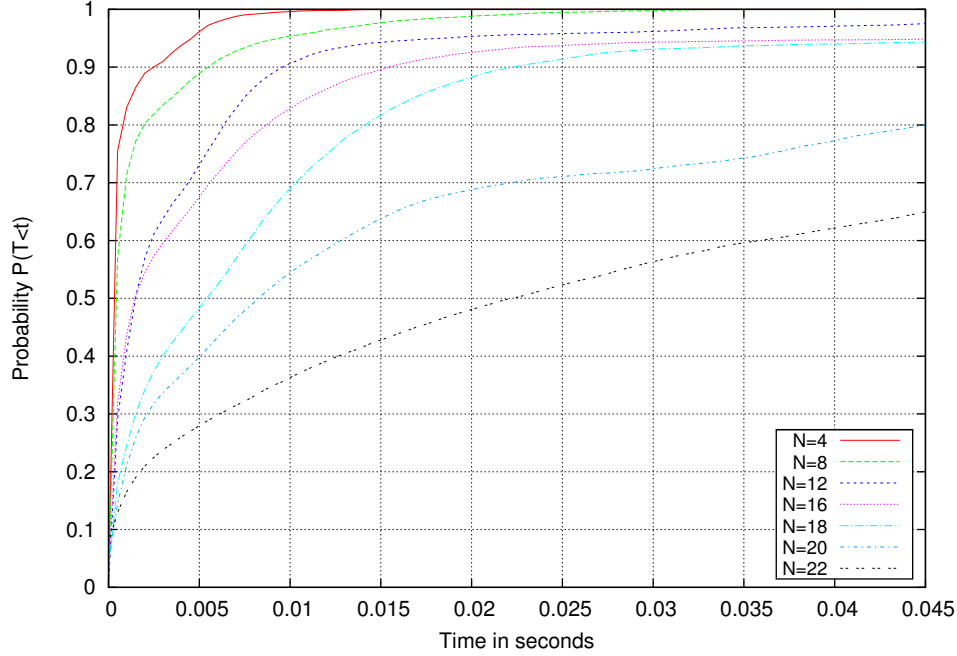


Figure 5.3: CDF of end-to-end frame delay

received frames only. As seen from Fig 5.3, the end-to-end delay gradually increases as N increases. It was seen that the average end-to-end frame delay stays under 0.025 seconds for N up to 20. Hence for the given network, the end-to-end frame delay has negligible impact on video quality as compared to the end-to-end frame loss.

Fig 5.4 depicts the average end-to-end frame loss in the network. The frame loss remains relatively low at up to 1.5% for up to 16 simultaneous video flows. Increasing N beyond 16 results in gradual increase in end-to-end frame loss with it reaching up to 7% at $N=22$. Also, it was seen that the average frame loss for I and P frames in the network was about the same.

Although the packet loss, end-to-end frame delay and frame loss observations indicate the degradation of video flows in the network as N rise, we still need an application layer metric to assess the video quality in the network. Fig 5.5 presents the average PSNR of all the video flows in the network with respect N . With an

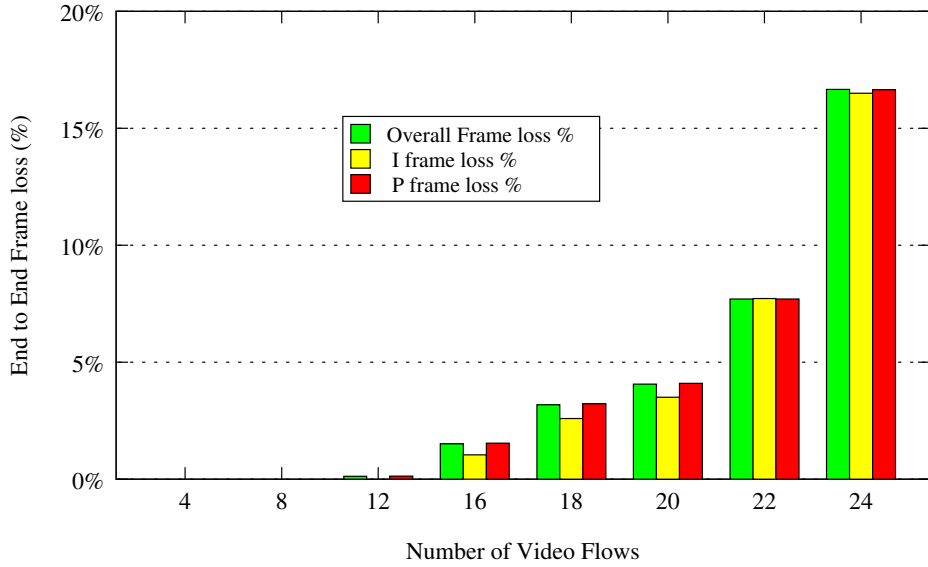


Figure 5.4: End-to-end frame loss vs. number of video flows

increase in N , the average PSNR decreased. The corresponding average MOS with respect to N is shown in fig 5.6. The MOS also decreases with an increase in the number of video flows. As indicated previously, all MOS and PSNR comparisons are done with respect to the transmitted video.

Fig. 5.7 depicts how the average MOS seen in the network is distributed in terms of frames with different MOS values. This distribution represents the distribution of MOS of all the frames belonging to all the videos and not the MOS of the videos themselves. As seen from Fig. 5.7, the proportion of "excellent" frames starts to gradually decrease with an increase in N . At $N=18$, the combined proportion of "poor", "bad" and "fair" is at 14.46% whereas it rises 16.77% at $N=20$. From Fig 5.6, it can be seen that the MOS values seem to indicate "good" video quality up to $N=20$, however such a high proportion of poor and bad frames results in unacceptable video quality overall even though the final average MOS is closer to 4. Hence, it was observed that the average MOS value doesn't portray the complete picture. For

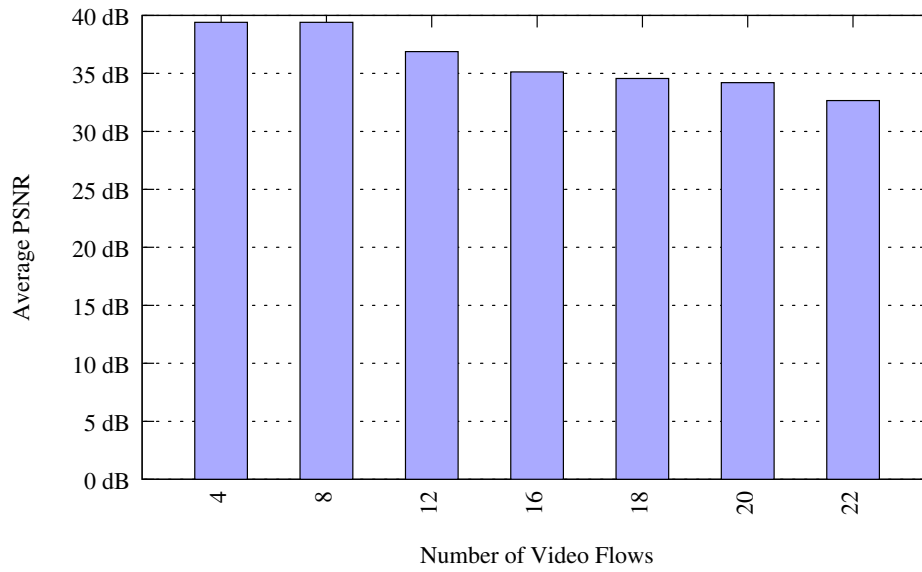


Figure 5.5: Average PSNR vs. number of video flows

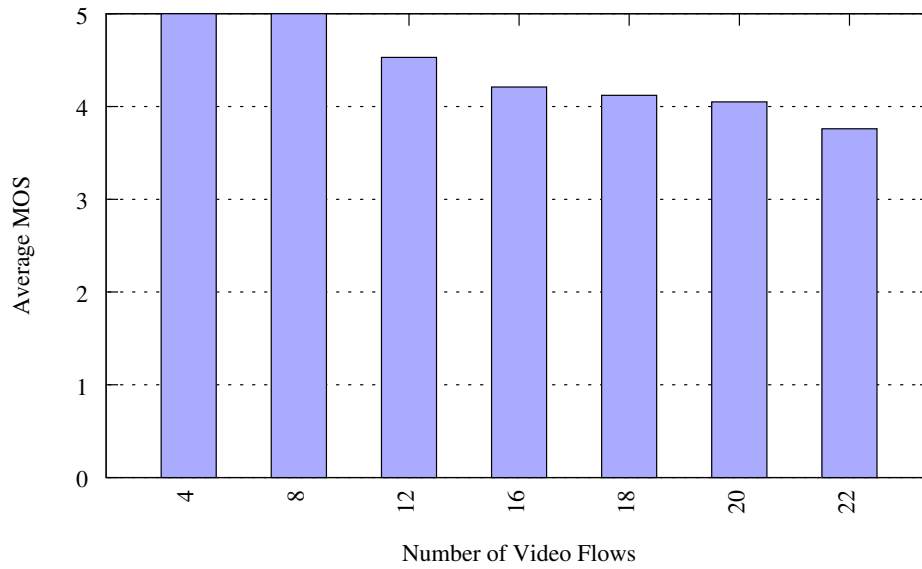


Figure 5.6: Average MOS vs. number of video flows

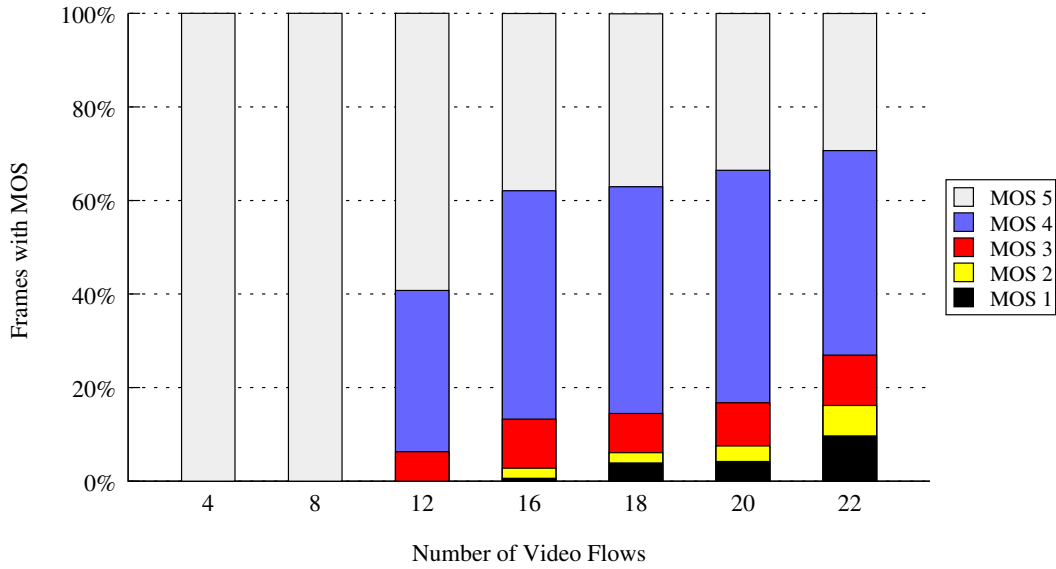


Figure 5.7: Distribution of frames with different MOS vs. number of video flows

example, if a steady video flow suddenly has a number of consecutive packet drops, the MOS for these frames will be bad but still the video can have an overall average MOS score in the good to excellent quality range. Fig. 5.6 in conjunction with Fig. 5.7 gives a clearer view of the video quality observed in the network.

Fig. 5.8 shows the proportion of frames with different MOS values observed per video flow in a N video flow scenario. The bar represents the mean value while the upper and lower error bars represent the highest and the lowest values observed among all the flows in the scenario. As mentioned above, since "poor" and "bad" quality frames severely impact the perceived video quality, it is necessary to specially observe the variation of this proportion of "poor" and "bad" frames among the video flows. From Fig. 5.8, it is seen that at $N=16$, when the network is nearing congestion, the deviation of this values among the different flows is less as compared to $N=18$ and higher values, when the network is congested. This disparity between the highest and lowest proportions observed as N increases indicates that different video flows start

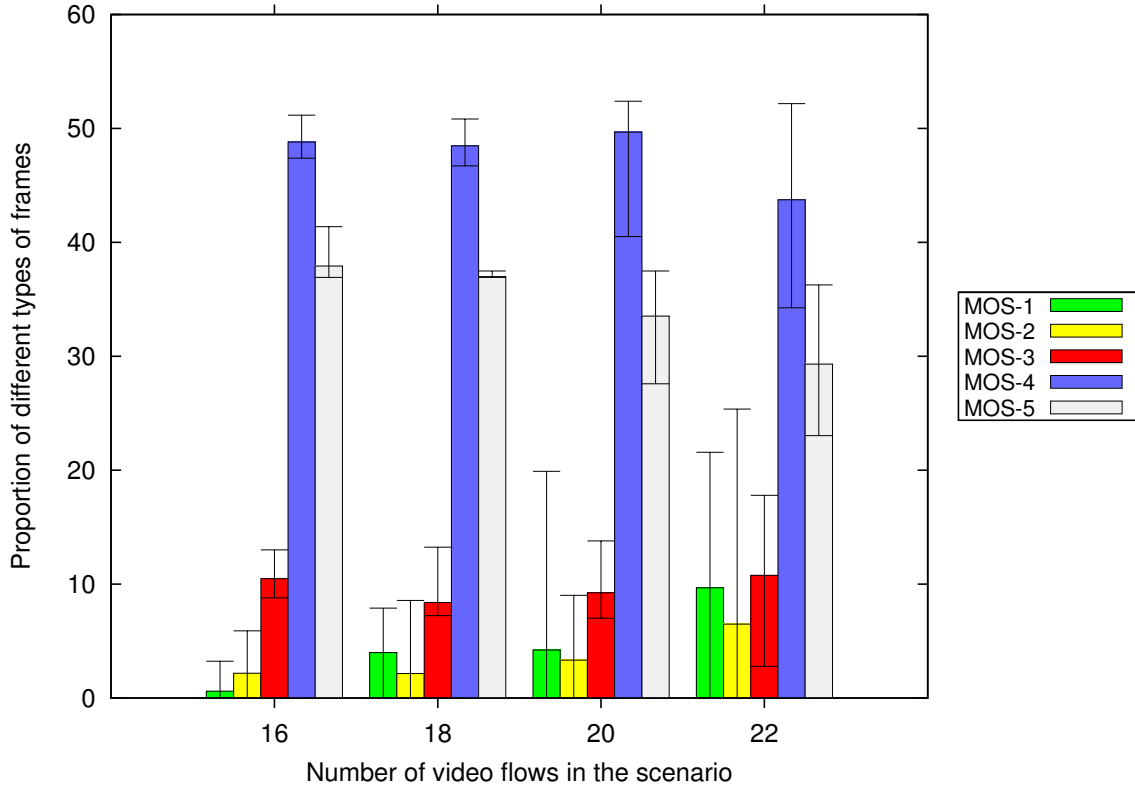


Figure 5.8: Proportion of frames with different MOS values

to observe different degree of perceived video quality in the same network. Hence, it is seen that all nodes do not get fair treatment once the network nears saturation and fairness becomes an issue in the network.

5.2 Change in Contention Window

From link layer observations, it is clear that the network saturates due to congestion at the MG due to traffic aggregation. In this section, we study the network and video performance when the contention window (CW) for the MG is decreased with respect to the MRs to relieve the congestion at the MG. As a result, packets in the queue at the MG have a statistically greater chance of selecting a random timer

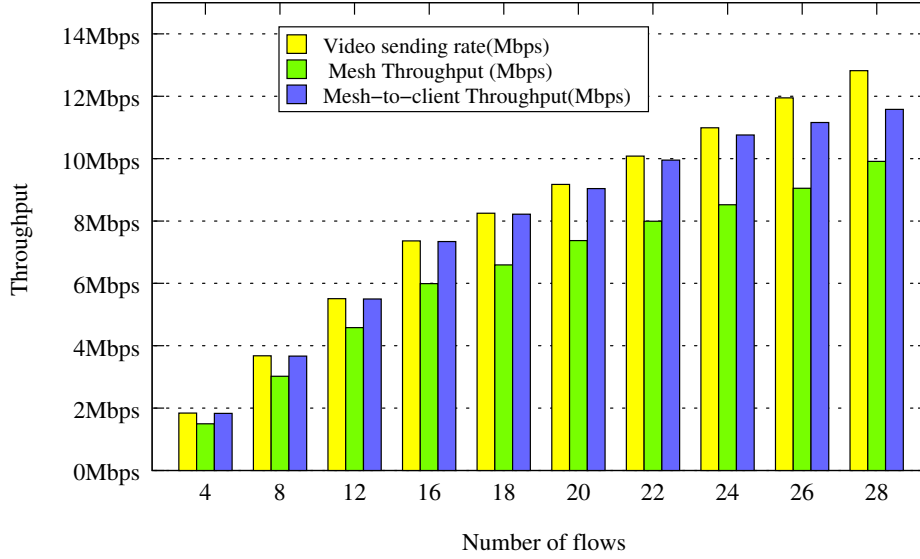


Figure 5.9: Throughput for CW change scenario

value that is lower than packets in the queue at the MRs.

In IEEE 802.11 distributed coordination function (DCF), the random back-off value is uniformly chosen from the interval defined in the contention window. Decreasing the contention window for the gateway in our topology would mean that the MG would have preferential and higher probability of access to the wireless medium than other nodes in its Carrier Sensing (CS) range. The standard values of minimum Contention Window (CW_{min}) and maximum Contention Window (CW_{max}) depends on the type of the PHY layer and for IEEE 802.11b/g radios are 31 and 1023 respectively. In 802.11e, the CW_{min} and CW_{max} values for video traffic for orthogonal frequency division multiplexing (OFDM) are set to 7 and 15 respectively. We choose a representative value close to this and the CW_{min} and CW_{max} for the MG were modified to 7 and 31 respectively whereas for the MRs, it was set to 31 and 1023. This allows MG to have exclusive access to the medium in case the mesh channel becomes idle.

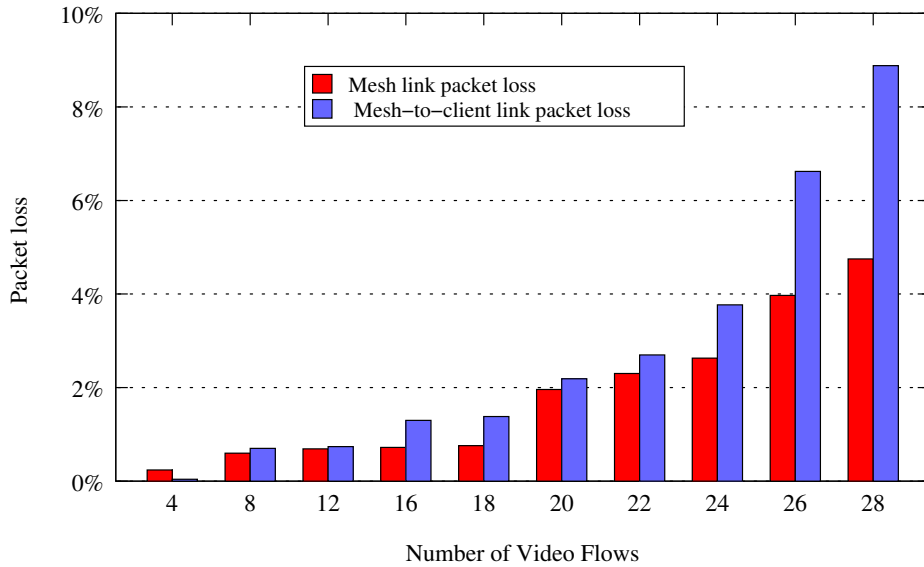


Figure 5.10: MAC layer packet loss for CW change scenario

Fig. 5.9 and Fig. 5.10 present the throughput and average MAC layer packet drop in the network. It can be seen from the figures that giving preferential access to the MG in this network architecture over the MRs results in an increase in throughput performance in the network. With the MG having less to wait than the MRs in the network to access the mesh channel, the MG is able to relieve the congestion that was seen in the original scenario. With this congestion window changed for the MG, we observe that up to 28 MCs can be accommodated by the network.

The average MAC layer packet drop percentage also dropped significantly with only 2.63% drop even at $N=24$ whereas in the original scenario, the drop was around 7.6%. It is also observed that as a result of more traffic passing on to the mesh-to-client channel from the mesh channel, the packet drops at the MAC layer for the mesh-to-client channel increased significantly as compared to the original scenario. In the original scenario as earlier mentioned, more than 90% of the packet drops occurred at the MG itself. In this case, as the traffic on the mesh-to-client channel

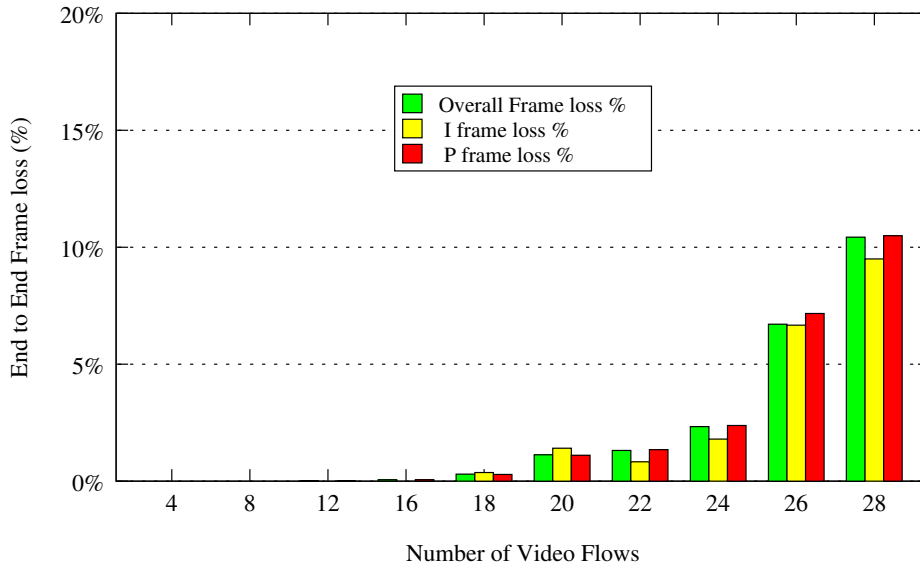


Figure 5.11: Frame loss for CW change scenario

increased, the queue drops and collisions were more prevalent on the mesh-to-client channel as compared to the mesh channel.

The corresponding frame loss graph and CDF for end-to-end delay for this scenario is depicted in Fig. 5.11 and Fig. 5.12 respectively. The frame loss rate also improves than the original scenario with the overall frame loss at around 1.31% even at $N=22$ as compared to 7.7% in the original scenario. The end-to-end frame delay was also seen to be more consistent with over 90% of successfully transmitted frames showing delays of less than 0.015 seconds at $N=22$.

The improvement in the overall quality of video flows is confirmed by Fig. 5.13 and Fig. 5.14 with the average MOS at $N=22$. Fig. 5.15 shows the MOS distribution for this scenario. In the original scenario, the network was able to support up to 20 video flows with the constraint of the average MOS being 4. In this case, up to 26 videos can be supported with the same constraint. More importantly, we see that the combined proportion of frames with MOS-1 and MOS-2 is less at $N=26$ in this case

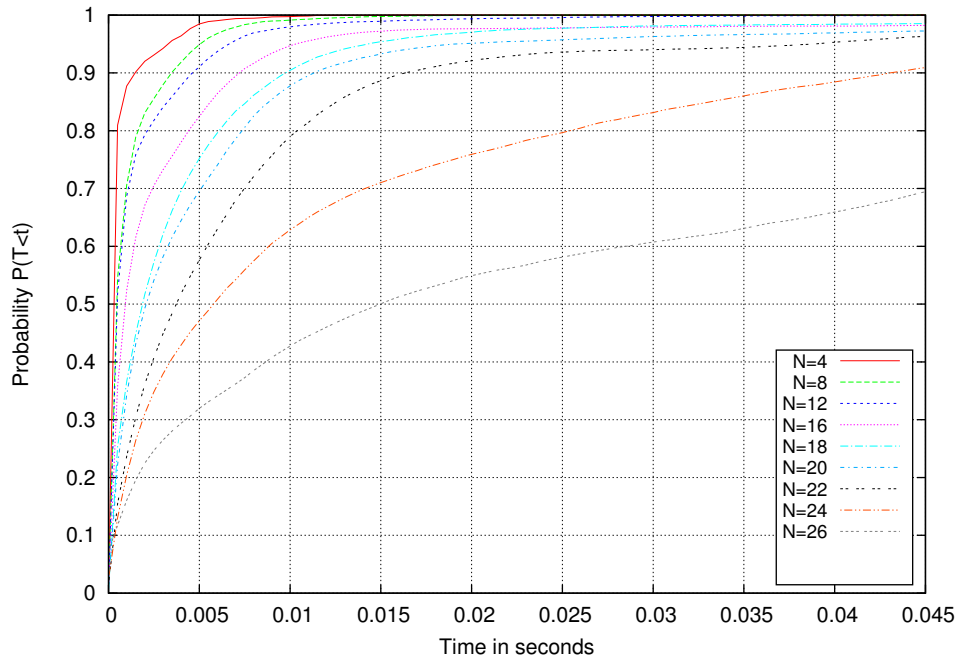


Figure 5.12: CDF for end-to-end frame delay CW change scenario

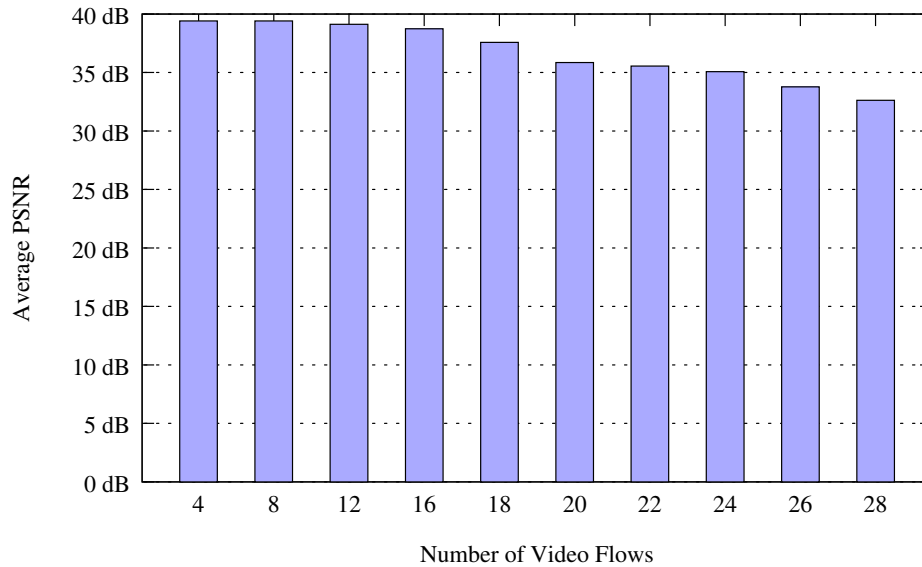


Figure 5.13: PSNR for CW change scenario

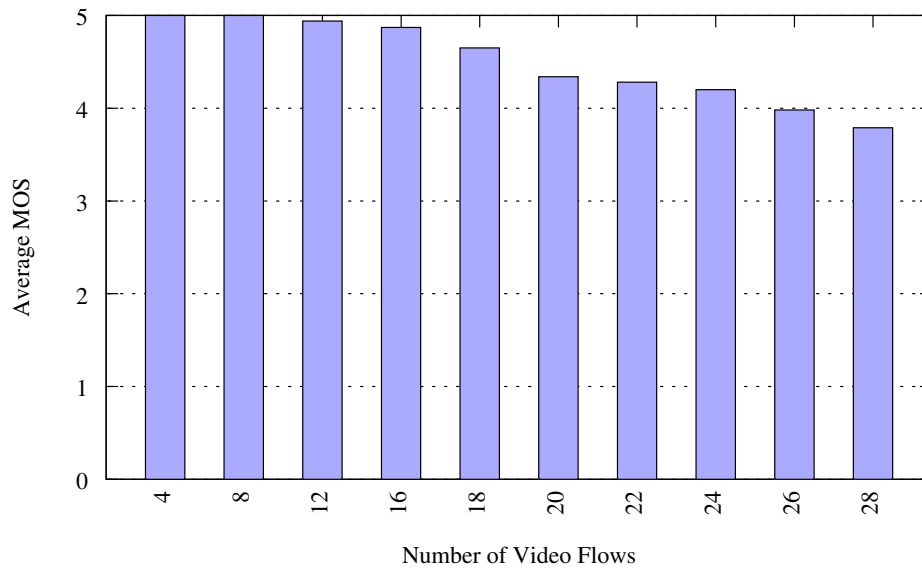


Figure 5.14: MOS for CW change scenario

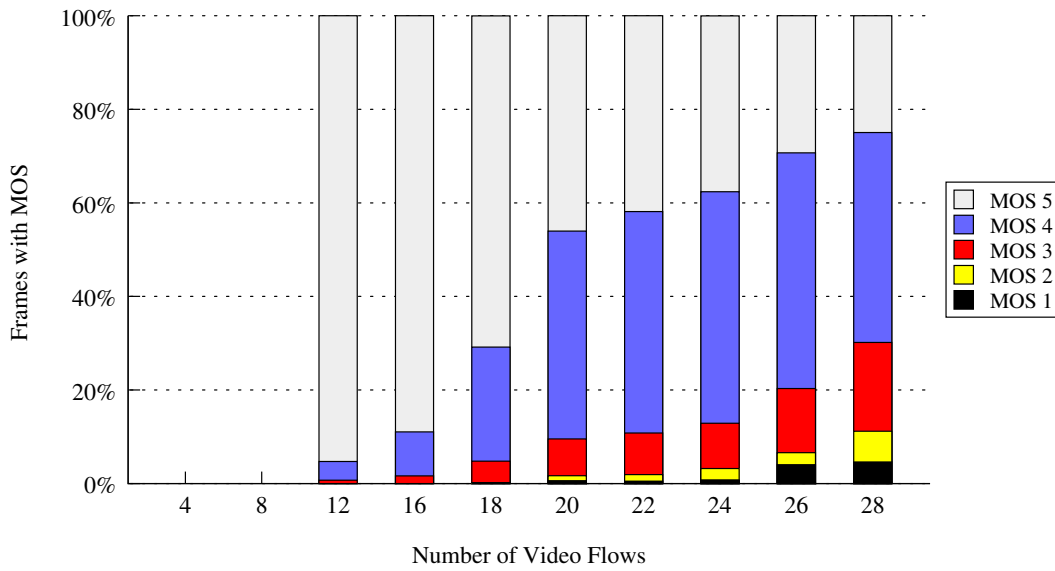


Figure 5.15: Distribution of frames with different MOS for CW change scenario

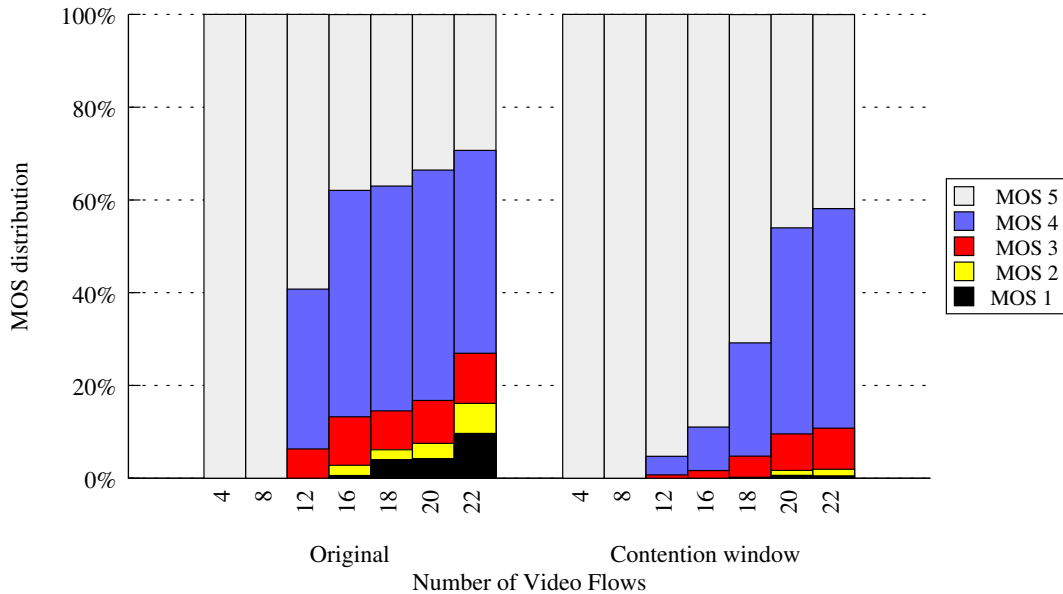


Figure 5.16: Comparison between original and CW change scenario

than at $N=20$ in the original scenario.

Fig. 5.16 summarize the average MOS and MOS distributions seen in the two scenarios.

5.3 Video Packet MTU Variation

In this section, we investigate how the packet size of the video traffic impacts the performance of the network. In the original case, the MTU for video packets was set to 1024 bytes. Two other packet MTU sizes viz. 512 bytes and 2048 bytes have been used for this scenario. In the initial scenario where the MTU was 1024 bytes, each video flow was composed of 2509 packets whereas in case 512 bytes MTU and 2048 bytes MTU, each flow was composed of 4625 packets and 1362 packets respectively.

The figures depicting throughput, packet loss, frame loss, average PSNR and

MOS for these packet sizes have been shown below side-by-side for easy comparison.

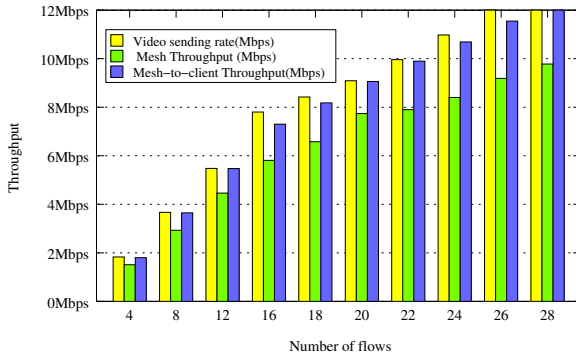


Figure 5.17: Throughput vs. number of video flows (2048 bytes MTU)

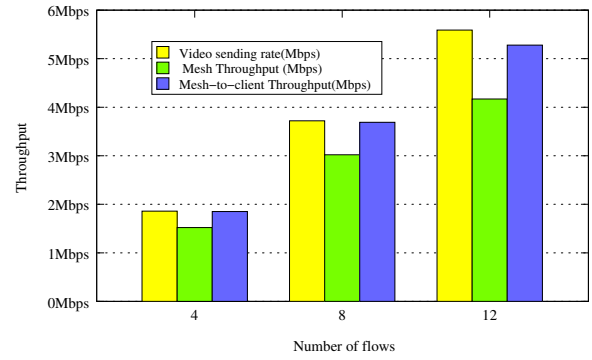


Figure 5.18: Throughput vs. number of video flows (512 bytes MTU)

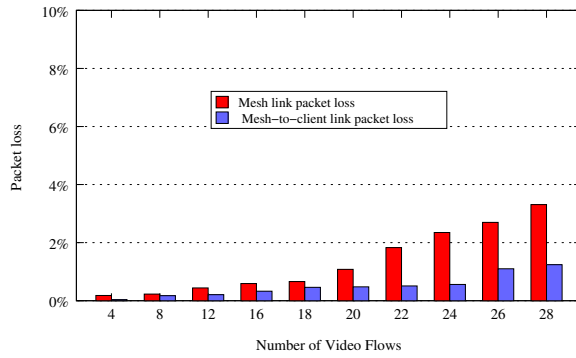


Figure 5.19: Average MAC layer packet loss (2048 bytes MTU)

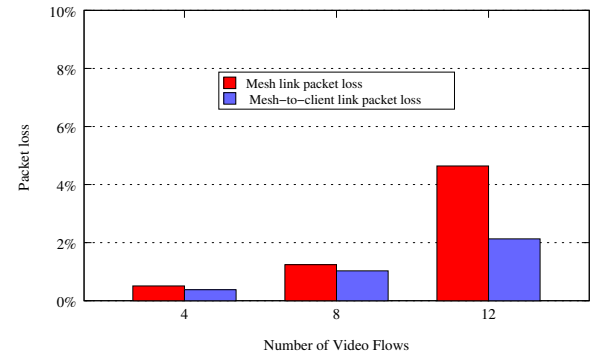


Figure 5.20: Average MAC layer packet loss (512 bytes MTU)

From figures 5.17 and 5.18, it can be seen that the network and video performance is greater for 2048 bytes packets. With a maximum packet size of 2048 bytes, the video stream contains lesser number of packets as compared to an MTU of 512 bytes. Hence, for a higher MTU, each node needs to access the medium less number of times as compared to a lower MTU and this results in less contention with other nodes in the network and an improvement in network performance. Also, the larger number of packets to be transmitted at a packet size of 512 bytes results in the network becoming quickly congested at the MG and the queue buffer being overflown

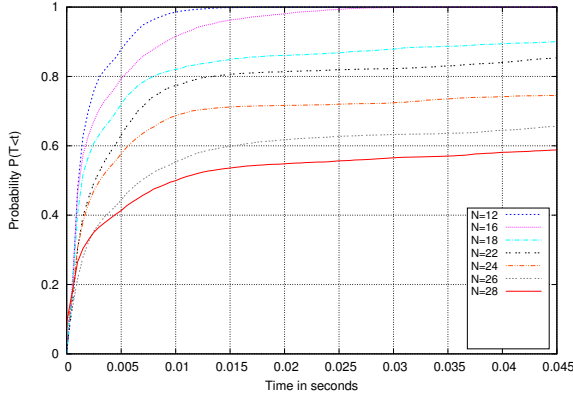


Figure 5.21: CDF for end-to-end frame loss (2048 bytes MTU)

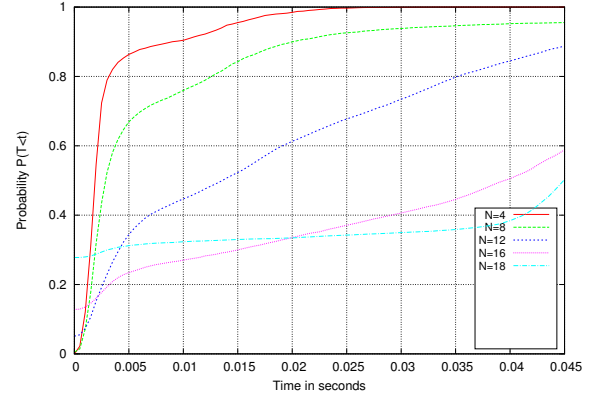


Figure 5.22: CDF for end-to-end frame loss (512 bytes MTU)

at the MG. Even at $N=12$, the network gets easily congested at the MG with over 4% packet loss observed at the MAC layer on the mesh channel. The packets lost due to a congested queue at the MG contributed to more than 90% of the packets dropped on the mesh channel. On the other hand, the reduced number of packets allows the network to easily support up to 26 video flows with just a packet loss of 2.6% at the MAC layer as seen from Fig 5.21.

The maximum MTU size change does result in a higher PER seen in the network which is around 3.5% for 2048 bytes as compared to 2.1% for 512 bytes but the impact of the PER is largely offset by the relatively lower MAC layer packet loss. This is also evident in the corresponding end-to-end frame loss figures 5.25 and 5.26.

We observe that for MTU equal to 2048 bytes, the same network is able to support up to 26 video flows whereas it supports just 8 video flows when MTU size is 512 bytes. The MOS dependency on number of flows in both scenarios are depicted in figures 5.27 and 5.28 respectively.

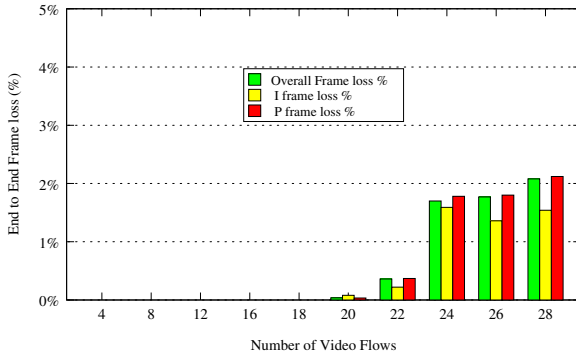


Figure 5.23: End-to-end frame loss (2048 bytes MTU)

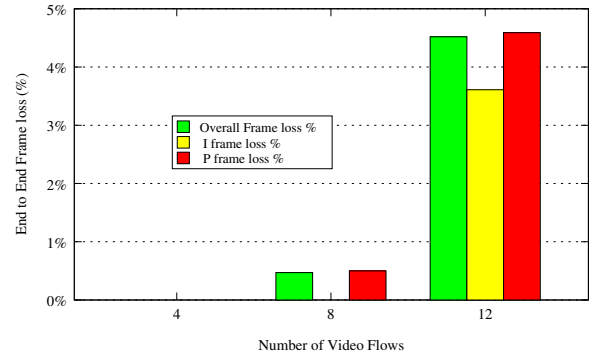


Figure 5.24: End-to-end frame loss (512 bytes MTU)

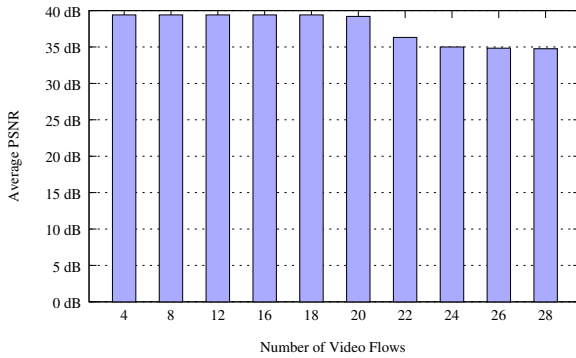


Figure 5.25: PSNR vs. number of flows (2048 bytes MTU)

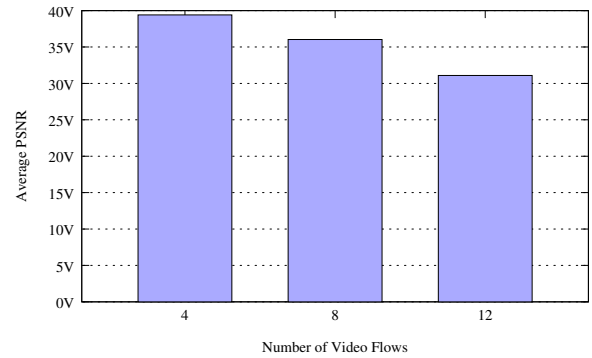


Figure 5.26: PSNR vs. number of flows (512 bytes MTU)

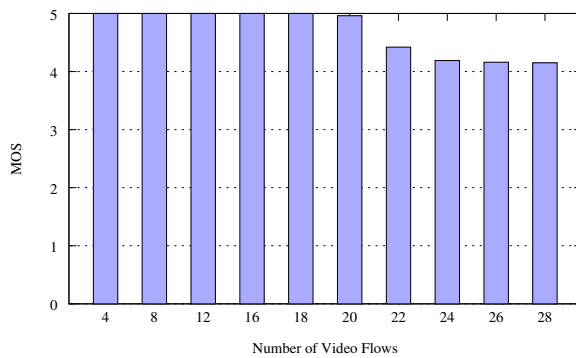


Figure 5.27: MOS vs. number of flows (2048 bytes MTU)

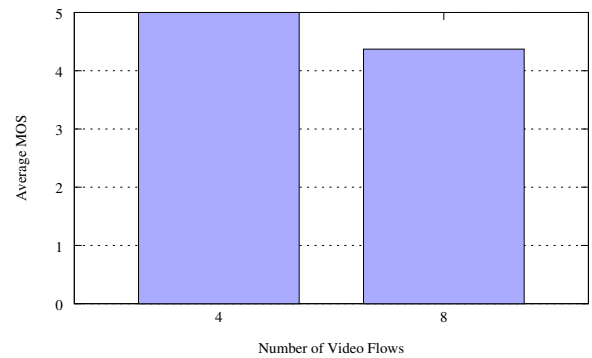


Figure 5.28: MOS vs. number of flows (512 bytes MTU)

Chapter 6

Conclusions and Future Work

This thesis evaluates the network and video streaming performance of a vehicle network with an infrastructure WMN backhaul. The network architecture consists of a number of MRs forming the mesh backhaul and providing connectivity to a number of MCs traversing the network and streaming video traffic from a server on the core network. Two separate IEEE 802.11g radios operating in orthogonal channels are used for mesh-to-mesh communication and mesh-to-client communication. The proposed routing protocol facilitates seamless handover of MCs within each routing zone in the network. The network and video streaming performance for each routing zone was evaluated with respect to the number of MCs in the zone.

In the first part of the evaluation, it was seen that the overall network performance decreased with an increase in the number of video flows. Throughput, link layer packet loss, end-to-end delay and end-to-end frame loss are evaluated and explained along with application layer metrics PSNR and MOS to observe the video performance in the network. The congestion at the MG is seen to be the main bottleneck in the given network architecture due to traffic aggregation at the gateway. Contention window parameters and the application packet size were varied to observe

their impact on the performance. The contention window for the gateway in the network was decreased compared to the MRs to relieve the congestion at the gateway. It is seen that giving preferential access to the MG in such network architecture resulted in up to 24 video flows being supported by the network as compared to 16 in the original scenario. Also, it is observed that the mesh-to-client channel became the bottleneck instead of the mesh channel in the network in this scenario as the number of video flows is increased. Two different packet MTU sizes viz. 512 bytes and 2048 bytes are used to observe their impact on the network. It is observed that larger packet sizes resulted in improved overall network and video performance in the network. The number of video flows supported in the network was seen to increase from 8 at an MTU of 512 bytes to 26 at an MTU of 2048 bytes.

Different hop lengths and topologies such as grid topologies have not been explored in this study and remain a topic for future work. The implemented simulation framework can also be extended for implementation and study of cross-layer adaptation mechanisms in the network for optimizing video streaming in described networks also remains a topic for future work in this area.

Appendices

Appendix A Simulation Framework Setup

A.1 NS-MIRACLE

NS-MIRACLE is one of the two external dynamic libraries that were integrated with ns-2 for the purpose of meeting certain simulation requirements. The proposed routing mechanism was implemented in NS-MIRACLE on top of the AODV code in the NS-MIRACLE beta release version. NS-MIRACLE is an external library that enhances the functionalities of ns-2 by adding features such as cross-layer messaging, enabling multiple modules in a single layer of the protocol stack etc. Features that were specifically enabled by adding ns-2 are support for multiple channels and multiple interfaces for a single node and also cross layer messaging.

A.2 dei80211.mr : Multi-rate library

The dei80211mr multi-rate library is a dynamic library that is available for NS-2 versions from ns-2.33 and above. The library enables us to capture realistic wireless channel properties and enables essential features such as multiple PHY modes or modulation schemes, multiple link rates, rate adaptation schemes and SINR based packet error model. All these features were used in our study to simulate modern mobile networks as NS-2 by default lacks any such implementation. Traditionally in ns-2, the RX Threshold variable was used to determine if a packet has been successfully received or not and this has been removed in favour of a SINR-based packet-level error model. Each received packet is evaluated individually with the received signal strength, noise and interference levels taking into account the packet capture effect. A pre-defined PER-SNR packet size based table is then used to determine the packet error probability based on the SINR for that packet. The standard installation comes

preinstalled with such table for both 802.11b and 802.11g. In case of collision, any colliding packets are treated as interference at the receiving end. Additional details for this dynamic library can be found in [27]

Bibliography

- [1] I.F. Akyildiz. A survey on wireless mesh networks. *IEEE Communications Magazine*, 43(9):S23–S30, September 2005.
- [2] Rahul Amin. An Integrated Routing and Distributed Scheduling Approach For Hybrid IEEE 802.16E Mesh Networks For Vehicular Broadband Communications. Master’s thesis, 2008.
- [3] Rahul Amin, Kuang-Ching Wang, and Parmesh Ramanathan. An Integrated Routing and Scheduling Approach for Persistent Vehicle Communication in Mobile WiMAX Mesh Networks. *MILCOM 2007 - IEEE Military Communications Conference*, pages 1–7, October 2007.
- [4] Y. Andreopoulos, N. Mastronarde, and M. Van Der Schaar. Cross-Layer Optimized Video Streaming Over Wireless Multihop Mesh Networks. *IEEE Journal on Selected Areas in Communications*, 24(11):2104–2115, November 2006.
- [5] Cagdas Atici and M. Oguz Sunay. Improving the performance of wireless H.264 video broadcasting through a cross-layer design. *2009 IEEE International Symposium on Broadband Multimedia Systems and Broadcasting*, pages 1–6, May 2009.
- [6] John Bicket, Daniel Aguayo, Sanjit Biswas, and Robert Morris. Architecture and evaluation of an unplanned 802.11b mesh network. In *Proceedings of the 11th annual international conference on Mobile computing and networking*, MobiCom ’05, pages 31–42, New York, NY, USA, 2005. ACM.
- [7] Maurizio Bonuccelli, Gaetano Giunta, Francesca Lonetti, and Francesca Martelli. Real-time video transmission in vehicular networks. *2007 Mobile Networking for Vehicular Environments*, pages 115–120, 2007.
- [8] Vincent Chavoutier, Daniela Maniezzo, Claudio E Palazzi, and Mario Gerla. Multimedia over Wireless Mesh Networks : Results from a Real Testbed Evaluation. *Network*, pages 56–62, 2007.

- [9] Xiaolin Cheng, Prasant Mohapatra, Sung-Ju Lee, and Sujata Banerjee. Performance evaluation of video streaming in multihop wireless mesh networks. *Proceedings of the 18th International Workshop on Network and Operating Systems Support for Digital Audio and Video - NOSSDAV '08*, page 57, 2008.
- [10] N. Cranley and M. Davis. Study of the Behaviour of Video Streaming over IEEE 802.11b WLAN Networks. *IEEE International Conference on Wireless and Mobile Computing, Networking and Communications, 2006. (WiMob'2006)*, pages 349–355, 2006.
- [11] Nicola Cranley and Mark Davis. Performance evaluation of video streaming with background traffic over IEEE 802.11 WLAN networks. *Proceedings of the 1st ACM workshop on Wireless multimedia networking and performance modeling - WMuNeP '05*, page 131, 2005.
- [12] dei80211mr: a new 802.11 implementation for NS-2. <http://www.dei.unipd.it/wdyn/?idsezione=5090>.
- [13] ffmpeg. <http://www.ffmpeg.org>.
- [14] Cisco Visual Networking Index: Forecast and 2010-2015 Methodology, June 2011.
- [15] I. Haratcherev, K. Langendoen, R. Laendijk, and H. Sips. Link adaptation and cross-layer signaling for wireless video-streaming in a shared medium. *2005 International Conference on Wireless Networks, Communications and Mobile Computing*, pages 1522–1526, 2005.
- [16] L. Haratcherev, J. Taal, K. Langendoen, R. Lagendijk, and H. Sips. Optimized video streaming over 802.11 by cross-layer signaling. *IEEE Communications Magazine*, 44(1):115–121, January 2006.
- [17] Hung-Chin Jang and Yu-Ti Su. A Hybrid Design Framework for Video Streaming in IEEE 802.11e Wireless Network. *22nd International Conference on Advanced Information Networking and Applications (aina 2008)*, pages 560–567, 2008.
- [18] Jens-Rainer-Ohm. Bildsignalverarbeitung fuer multimedia-systeme, Skript, 1999.
- [19] S Khan, Y Peng, E Steinbach, M Sgroi, and W Kellerer. Application-driven cross-layer optimization for video streaming over wireless networks. *IEEE Communications Magazine*, 44:122–130, 2006.
- [20] S Khan, Y Peng, E Steinbach, M Sgroi, and W Kellerer. Optimization for Video Streaming over Wireless Networks. *IEEE Communications Magazine*, (January):122–130, 2006.

- [21] Jirka Klaue, Berthold Rathke, and Adam Wolisz. EvalVid - A Framework for Video Transmission and Quality Evaluation. *Computer Performance*, (September), 2003.
- [22] a. Ksentini, M. Naimi, and A. Gueroui. Toward an improvement of H.264 video transmission over IEEE 802.11e through a cross-layer architecture. *IEEE Communications Magazine*, 44(1):107–114, January 2006.
- [23] Feng Li, Jae Chung, Mingzhe Li, Huahui Wu, Mark Claypool, and Robert Kinicki. Application , Network and Link Layer Measurements of Streaming Video over a Wireless Campus Network. *Methodology*, pages 1–14.
- [24] Mingzhe Li, Feng Li, Mark Claypool, and Robert Kinicki. Weather Forecasting - Predicting Performance for Streaming Video over Wireless LANs. *Weather and Forecasting*, pages 33–38, 2005.
- [25] A. Majumda, D. G. Sachs, I. V. Kozintsev, K. Ramchandran, and M. M. Yeung. Multicast and unicast real-time video streaming over wireless LANs. *Circuits and Systems for Video Technology, IEEE Transactions on*, 12(6):524–534, 2002.
- [26] N. H. Moleme, M. O. Odhiambo, and A. M. Kurien. Improving Video Streaming over IEEE 802.11 Mesh Networks through a Cross-Layer Design Technique. *2008 Third International Conference on Broadband Communications, Information Technology & Biomedical Applications*, pages 50–57, 2008.
- [27] N. H. Moleme, M.O. Odhiambo, and A.M. Kurien. Enhancing video streaming in 802.11 Wireless Mesh Networks using two-layer mechanism solution. *Africon 2009*, (September):1–6, September 2009.
- [28] The Network Simulator ns 2. <http://www.isi.edu/nsnam/ns/>.
- [29] ns-MIRACLE: Multi InteRface Cross Layer Extension for ns 2. <http://www.dei.unipd.it/ricerca/signet/tools/nsmiracle>.
- [30] J Ott. Drive-thru Internet: IEEE 802.11 b for automobile users. *Third Annual Joint Conference of the IEEE*, 2004.
- [31] Eric Setton, Taesang Yoo, Xiaoqing Zhu, Andrea Goldsmith, and Bernd Girod. Cross-layer design of ad hoc networks for real-time video streaming. *IEEE Wireless Communications Magazine*, 12:59–65, 2005.
- [32] Irfan Sheriff, Kevin C. Almeroth, Yuan Sun, and Elizabeth M. Belding-Royer. An Experimental Study of Multimedia Traffic Performance in Mesh Networks. *Traffic*, pages 25–30.

- [33] Guojun Shui and Shuqun Shen. Video Streaming Transmission Over Multi-Channel Multi-Path Wireless Mesh Networks. *2008 4th International Conference on Wireless Communications, Networking and Mobile Computing*, pages 1–4, October 2008.
- [34] Yusuke Takahashi, Yasunori Owada, Hiraku Okada, and Kenichi Mase. A wireless mesh network testbed in rural mountain areas. In *Proceedings of the second ACM international workshop on Wireless network testbeds, experimental evaluation and characterization*, WinTECH '07, pages 91–92, New York, NY, USA, 2007. ACM.
- [35] Intel technology powers in-car infotainment system from BMW individual. <http://www.intel.com/business/enterprise/emea/eng/casestudies/all/271119.htm>, March 2007.
- [36] An Introduction to Wireless Mesh Networking. <http://www.firetide.com>, March 2005.
- [37] EvalVid A Video Quality Evaluation Tool-set. <http://www.tkn.tu-berlin.de/research/evalvid/>.
- [38] Hao Wang, Andras Farago, and Subbarayan Venkatesan. Video Streaming Over Multi-hop Wireless Networks. *Seventh IEEE International Symposium on Multimedia (ISM'05)*, pages 624–629.
- [39] Dapeng Wu, Yiwei Thomas Hou, Wenwu Zhu, Hung-ju Lee, Tihao Chiang, Yaqin Zhang, and H Jonathan Chao. On End-to-End Architecture for Transporting MPEG-4 Video over the Internet. 2000.
- [40] Fei Xie, Kien a. Hua, Wenjing Wang, and Yao H. Ho. Performance Study of Live Video Streaming Over Highway Vehicular Ad Hoc Networks. *2007 IEEE 66th Vehicular Technology Conference*, pages 2121–2125, September 2007.
- [41] Xiaoqing Zhu, Bernd Girod, and Peter Van Beek. Distributed channel time allocation and rate adaptation for multi-user video streaming over wireless home networks. In *IEEE International Conference on Image Processing (ICIP07)*, pages 69–72, 2007.